UNIVERSIDADE FEDERAL DO RIO GRANDE DO SUL
ESCOLA DE ENGENHARIA
DEPARTAMENTO DE METALÚRGIA
TRABALHO DE DIPLOMAÇÃO

ISO-VISCOSITY CURVES FOR SECONDARY STEELMAKING SLAGS IN THE CaO-SiO_2-Al_2O_3-MgO SYSTEM AT TEMPERATURES 1500,1600 AND 1700 °C

TRABALHO DE DIPLOMAÇÃO

AUGUSTO LACHINI PEREIRA

PORTO ALEGRE, RS
2021

UNIVERSIDADE FEDERAL DO RIO GRANDE DO SUL
ESCOLA DE ENGENHARIA
DEPARTAMENTO DE ENGENHARIA METALÚRGICA
TRABALHO DE DIPLOMAÇÃO

ISO-VISCOSITY CURVES FOR SECONDARY STEELMAKING SLAGS IN THE CaO-SiO_2-Al_2O_3-MgO SYSTEM AT TEMPERATURES 1500,1600 AND 1700 °C

AUGUSTO LACHINI PEREIRA

Trabalho de Diplomação apresentado como requisito parcial para obtenção do título de Engenheiro Metalúgico.

Orientador:
Prof. Wagner Viana Bielefeldt

Coorientador:
Prof. Jean-Philippe Harvey
Department of Chemical Engineering
Polytechnique Montréal

PORTO ALEGRE, RS
2021

Autor, Augusto Lachini Pereira
Iso-viscosity curves for secondary steelmaking slags in the CaO-SiO_2-Al_2O_3-MgO system at temperatures 1500,1600 and 1700°C / Augusto Lachini Pereira. -- 2021.
106 f.

Orientador: Wagner Viana Bielefeldt

Trabalho (Diplomação) - Universidade Federal do Rio Grande do Sul, Escola de Engenharia, Departamento de Engenharia Metalúrgica , Porto Alegre, BR-RS, 2021.

Viscosidade, Escórias de refino secundário, Termodinâmica computacional, FactSage 7.3 I. Wagner Viana Bielefeldt, orient. II. Jean-Philippe Harvey, coorient. III. Título.

"Somewhere, something incredible is waiting to be known"
— CARL SAGAN

Acknowledgments

Aos meus pais, pelo amor, incentivo e apoio incondicional. Agradeço em especial a minha mãe Lorena Lachini Pereira, companheira que me deu apoio, icentivo nas horas difíceis onde não via saída mas ela sempre acreditou e confiou em mim. Ao meu pai Carlos Aurélio Alves Pereira que sempre enfrentou barreiras para me proporcionar o melhor- saiba tu sempre me motivou a ser melhor e me dedicar ao máximo.

Aos que também são mãe e pai, eu agradeço a vocês Elaine Sieben Czuka, Lavínia Gloor Lachini e Augusto Benedito Czuka por me ajudarem sempre e enfrentarem as lutas comigo.

Aos meus que sempre foram um exemplo Arthur Lachini Pereira e Gustavo Coelho Fermino vos agradeço por sempre servirem como uma ispiração para mim.

To my advisor and co-advisor for their dedication to this work. To Professor Wagner Viana Bielefeldt, for his orientation, support and trust. To Professor Jean-Philippe Harvey (Polytechnique Montréal) for the opportunity and support in writing this work.

Ao Vinicius Cardoso da Rocha que me guiou a criar o trabalho acadêmico desde sempre.

A Universidade Federal do Rio Grande do Sul (UFRGS), pela oportunidade de fazer o curso. Ao Laboratório de Siderurgia da UFRGS (LaSid) por ser um ambiente criativo e amigável que proporciona.

A todos que direta ou indiretamente fizeram parte de minha formação, o meu muito obrigado.

Agradeço a Meylín Lourenço Pereira por eu tentar ser uma motivação e um

incentivo para te inspirar a buscar sempre um futuro melhor.

Resumo

Uma pequena alteração na composição química e na temperatura afeta a viscosidade da escória, a qual possui uma grande parte das propriedades físicas relativas às escórias de refinação. A optimização desses parâmetros pode afetar a limpeza do aço. O processo de medição da viscosidade é considerado custoso, portanto a relação custo-benefício não favorece as medidas a altas temperaturas. Como alternativa, é possível aplicar modelos matemáticos ou software termodinâmico para obter viscosidades para uma determinada gama de composição química e temperatura das escórias. O presente trabalho contempla uma validação dos dados experimentais, recolhidos na literatura, com dados calculados. E também propõe também uma representação precisa das curvas de iso-viscosidade aplicadas às escórias secundárias da siderurgia, cobrindo as gamas de composição: 0-100 massa.% CaO, 0-100 massa.% SiO_2, 0-100 massa.% Al_2O_3 e 0-15 massa.% MgO (CSAM) sistema a 1500ºC a 1700ºC. Os campos de representação de viscosidade incluem escória totalmente líquida e parcialmente líquida no sistema CSAM. As viscosidades foram calculadas utilizando o sotware *FactSage*. 7.3 (para Fase Líquida) e a equação *Roscoe-Einstein* com auxílio do *FactSage*. 7.3 (para Fase mistura) para um total de 15910 escórias. Os resultados preliminares indicaram que existe uma convergência significativa entre os dados das viscosidades calculadas e experimentais.

Palavras-chave: Viscosidade, Escórias de refino secundário, Termodinâmica computacional, FactSage 7.3

Abstract

A minor change in the chemical composition and temperature affects the slag viscosity, which has a great impact of the physical properties influencing refining slags. Optimizing those parameters may affect the steel cleanliness. The viscosity measurement process is considered expensive, so the cost-effectiveness does not favor the measures at high-temperatures. Alternatively, it is possible to apply mathematical models to calculate viscosities of slags for a given range of chemical composition and temperature. The present work presents a validation of the viscosity experimental data, collected in the literature, with calculated data via *FactSage* in this work. Also proposes an accurate representation of iso-viscosity curves applied for secondary steelmaking slags, covering the composition ranges: 0–100 wt.% CaO, 0–100 wt.% SiO_2, 0–100 wt.% Al_2O_3 and 0–15 wt.% MgO (CSAM) system at 1500ºC to 1700°C. The viscosity representation fields include fully liquid and partially liquid slag in the CSAM system. The viscosities were calculated using the *FactSage* 7.3 (for Liquid Phase) and the *Roscoe-Einstein* equation (for multiphasic systems) for a total of 15910 slags compositions. The preliminary results indicated that there is a significant convergence between the calculated and experimental viscosities data. It is promoting an efficient approximation of the iso-viscosity curves for the CSAM slag system in the high-temperatures.

Key-words: Viscosity, Steelmaking slags, Computational thermodynamics, FactSage 7.3

List of Figures

List of Tables

Symbols List

Δg_{AB}	Molar Gibbs Energy	$\frac{\mathrm{J}}{\mathrm{mol-K}}$
A_{Liquid}	Liquid metal oxide	–
A_{sol}	Solid metal oxide	–
Al	Aluminium	–
Al_2O_3	Oxide of Aluminium	–
B	Bismuth	–
B_{Liquid}	Liquid metal oxide	–
B_{sol}	Solid metal oxide	–
Ca	Calcium	–
CaF_2	Calcium fluoride	–
CaO	Oxide of Calcium	–
Cr	Chromium	–
Fe	Iron	–
FeO	Iron Oxide	–
K	Potassium	–
Mg	Magnesium	–
MgO	Oxide of Magnesium	–
MnO	Manganese oxide	–

Mo	Molybdenum	–
Na	Sodium	–
O	Oxygen	–
P	Phosphorus	–
Pb	Lead	–
Pt	Platinum	–
Rh	Rhodium	–
Si	Silicon	–
Si_4	Silicon Tetrahedron	–
SiO_2	Oxide of Silicon	–
T	Temperature	C
T_{liq}	Liquidus Temperature	C
T_{sol}	Solidus Temperature	C
T_{start}	Start Temperature	C
Ti	Titanium	–
V	Vanadium	–
X_{liq}	Liquid slab	–

Greek Letters

f	Solid fraction	–
δ	Average percent error	%
δ_i	Percent error	%
η	Effective viscosity	Pa s
η_l	Viscosity of liquid phase	Pa s

ρ	Solid interaction parameter	–

Oversubscribed

A	Acide oxides
B	Base oxides
Equilib	Equilib module of FactSage
FactPS	Database of FactSage
FToxid	Database of FactSage
Phase Mixture	Two phase slag - solid and liquid
Viscosity	Viscosity module of FactSage

Acronyms

CSAM	CaO - SiO_2 - Al_2O_3 - MgO *system*
MQM	*Modified Quasichemical model*
wt.%	*Weight percentage*

Contents

Chapter 1

Introduction

The viscous behavior of slags is of great importance in order to understand its physico-chemical properties, such as gas permeability, heat transfer, rate of desulphurization, and more. (PENGCHENG; XIAOJUN, 2016). Hence it is an essential properly to tune productivity and ensure optimum operations. For these reasons, for six decades, slag viscosities have been measured not only for theoretical research but also for the industrial applications (MACHIN; HANNA, 1945; MACHIN; YEE, 1948; MACHIN; YEE; HANNA, 1952; MACHIN; YEE, 1954; KOZAKEVITCH, 1954; KOZAKEVITCH, 1960; KOZAKEVITCH; MISRA, 1966; J.; M, 1995; SAITO et al., 2003; KIM et al., 2010; SONG; SHU; SICHEN, 2011; CHOPRA; TANEJA, 1964; URBAIN; BOTTINGA; RICHET, 1982; TANG et al., 2011; SHANKAR, 2007; FORSBACKA et al., 2007; GAO et al., 2014; SCHUMACHER; WHITE; DOWNEY, 2015).

Steelmaking slags conventionally contain CaO, SiO_2, Al_2O_3, MgO. Slags viscosity changes in a wide range depending on the temperature and composition. This quaternary system is composed of the most common oxides employed for steel refining (i.e. secondary metallurgy). In this case, the slag must be designed to present a maximum refining capacity. The viscosity directly affects the kinetics of the main refining reactions of steel by slag, including the removal of impurities such as sulfur (ROCHA et al., 2017) and nonmetallic

inclusions (ROCHA et al., 2017). Unfortunately, it is well known that high-temperature viscosity measurement is time-consuming and costly. Thus it is pf prime importance to predict the viscosity of applying models which enable calculation of viscosity for a wide range of composition and temperature.

Under specific conditions, steelmaking slags may be in equilibrium with solids, multiphasic system, in which it contains a liquid fraction and a solid fraction. Because of the difficulties in the measure most of two-phase system viscosity, researchers have been estimating the viscosity of solid-liquid mixtures using models. Einstein (EINSTEIN, 1906; EINSTEIN, 1911) derived a simple model to estimate the viscosities of two-phase systems and co-works (ROSCOE, 1952) improved the model. At the origin Einstein developed a model that could be applied only to small fractions of solid particles. Roscoe (ROSCOE, 1952) extended the model to large fractions of solid (XU, 2015).

1.1 Motivation and Objective

It is difficult to find in the literature viscosity data for multi-component slags at high temperature. For this reason, the motivation of this work is to generate graphs to aid and understand the viscosity behavior of slag. In turn, these graphs can used as tools to control metallurgical phenomena in secondary refining. The *FactSage* software has been used to calculate viscosity of these slags as well as the phase assemble for imposed conditions of temperature and compositions.

The present work aims to apply a mathematical viscosity model to the slags viscosities in the system CaO-SiO_2-Al_2O_3-MgO, (CSAM), for a temperature between 1500ºC - 1700 ºC. This study covers the following composition range 0–100 wt.% CaO, 0–100 wt.% SiO_2, 0–100 wt.% Al_2O_3 and 0–15 wt.% MgO

(CSAM) under these conditions, the system may be liquid (slag) or bi-phasic.

In addition, this work provides iso-viscosity curves for different CSAM slag systems for single-phase and multiphasic slags. The representation of iso-viscosity outside the single-phase slag of ternary diagrams at high temperatures is gaining more importance for many industrial steelmaking applications since slag contain solid fraction are commonly used for the refining of special steels. The other objectives are listed as follows:

- Calculate single-phase the viscosity using *FactSage* and estimate the viscosity of two-phase slags using the Roscoe-Einstein equation;
- Validate the *FactSage* viscosity model using experimental data collected in the literature;
- Construct graphical representations of iso-viscosity curves.

Chapter 2

Literature Review

This chapter will present a contextualization of the worldwide production of steel and it will also provide information about the Brazilian production. Subsequently, the processes and parameters related to steel production will be detailed. Finally a description of the structures and physico-chemical properties of steel slag and the use of thermodynamic software to virtual steelmaking process simulations will be provided.

2.1 World steel production and aspects of the Brazilian market

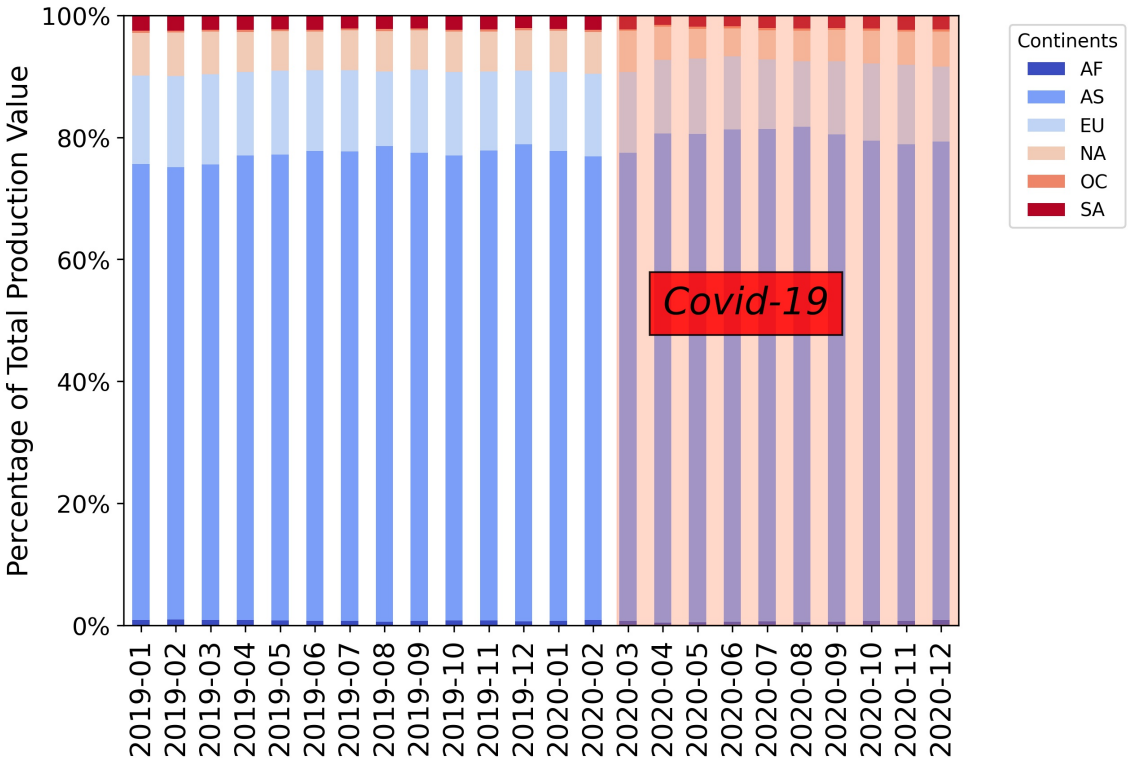

FIGURE 2.1. Crude Steel Production by Continents

According to the *World Steel Association* (2019), world crude steel production in 2019 reached the 1 846 391 thousands tons. A production decrease of 0.9% was observed in 2020 for the same period.

As shown in the Figure 2.1 since March 2020 there has been an increase in crude steel production on the Asian continent combined to a decrease in production on the other continents. This is due to the influence of the COVID-19

pandemic on crude steel production.

The 5 countries with the highest crude steel production in the Asian continent between 2019 and 2020 are:

1. China - 2054258 thousands tons

2. India - 206918 thousands tons

3. Japan - 182745 thousands tons

4. South Korea - 139034 thousands tons

5. Turkey - 69472 thousands tons

The Figure 2.2 represents crude steel production in the above countries between 01/2019 and 12/2020.

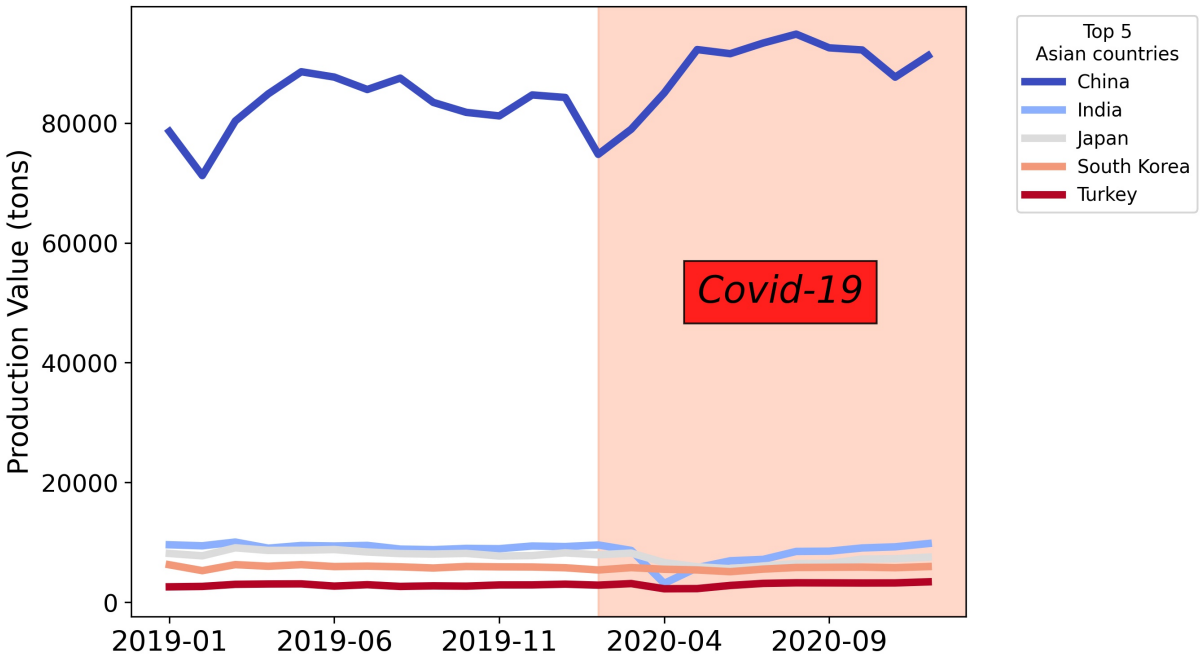

FIGURE 2.2. Crude Steel Production in the Top 5 Asian Countries

According to the Figure 2.2 it is possible to conclude that China had an increase in crude steel production from the beginning of the pandemic. This increase in crude steel production was already expected in previous years, but it grew more sharply and for longer than in previous years.

Now looking at the South American continent, the five countries with the largest crude steel production are:

1. Brazil - 63157 thousands tons
2. Argentina - 8296 thousands tons
3. Peru - 1992 thousands tons
4. Colombia - 2458 thousands tons

5. Chile - 2096 thousands tons

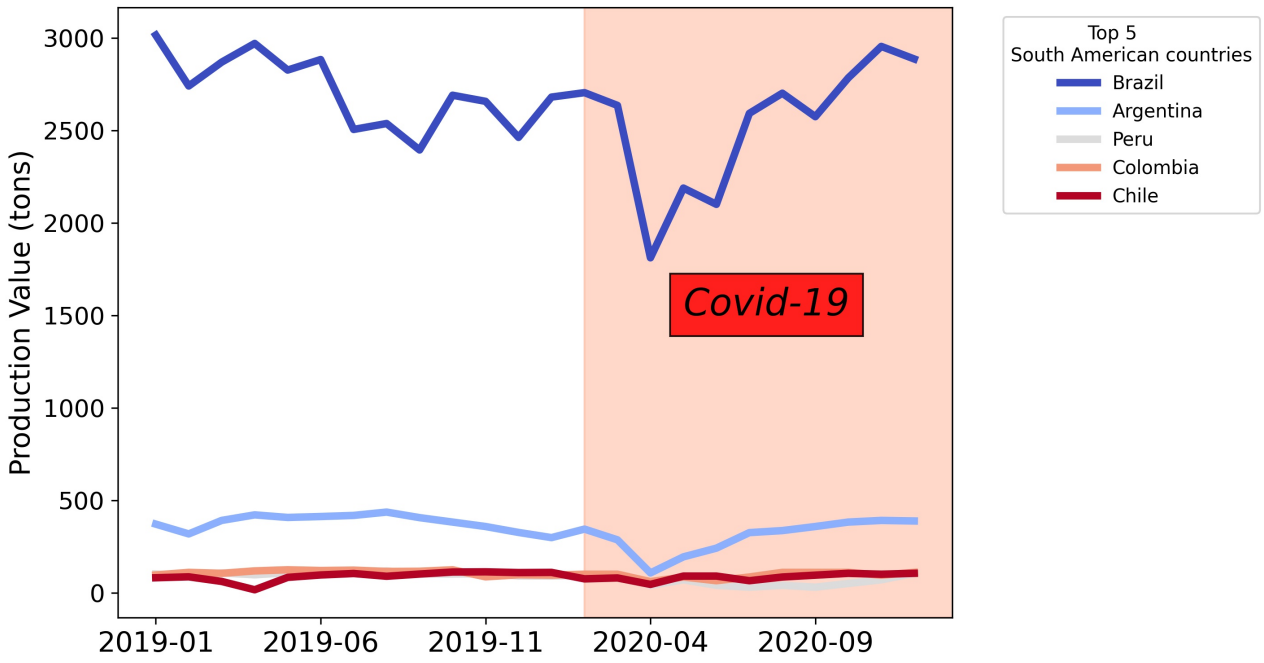

FIGURE 2.3. Crude Steel Production in the top 5 countries in South America

According to Figure 2.3 the beginning of the pandemic due to COVID-19 led a slowdown in the production of crude steel in Brazil (in "V" shape). However, production returned to normal in October 2020, with a production of 2800 thousand tons per month.

Finally looking at the North American continent, the five countries with the largest crude steel production:

1. United States - 159599 thousands tons

2. Mexico - 34770 thousands tons

3. Canada - 23607 thousands tons

4. Guatemala - 525 thousands tons

5. Cuba - 403 thousands tons

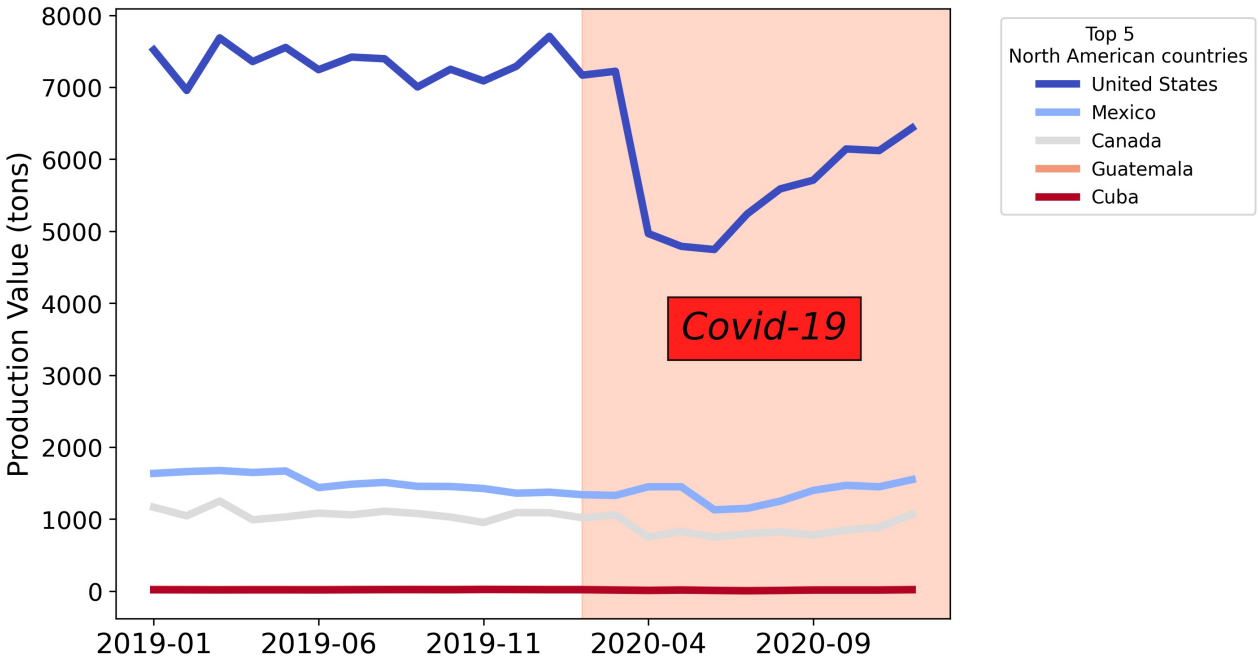

FIGURE 2.4. Crude Steel Production in the top 5 countries in Noth America

Figure 2.4 shows the influence of COVID-19 on crude steel production on the North American continent. It can be seen that the United States was the country that was the most impacted by COVID-19, as opposed to Mexico and Canada which were not as impacted.

2.2 Electric steelmaking

One of the steel production routes is by melting and refining scrap in electric arc furnaces. Steelmaking process that use electricity gain relevance in the steelmaking industry, because they are directly associated with the recycling of ferrous scrap and lead to a reduction in the exploitation of iron ore, coal and other raw materials. Besides this, there is a reduction of pollution (coming from the exhaust gas) from the reduction of iron ore.

The electric melt shop, in specialty steel mills, has several operational cells, namely the scrap yard, electric arc furnace (EAF), ladle furnace (LF), vacuum degasser (VD) and, finally, the continuous casting and/or conventional casting. Figure 2.5 represents a flowchart of the steelmaking process steps in an electric steelmaking.

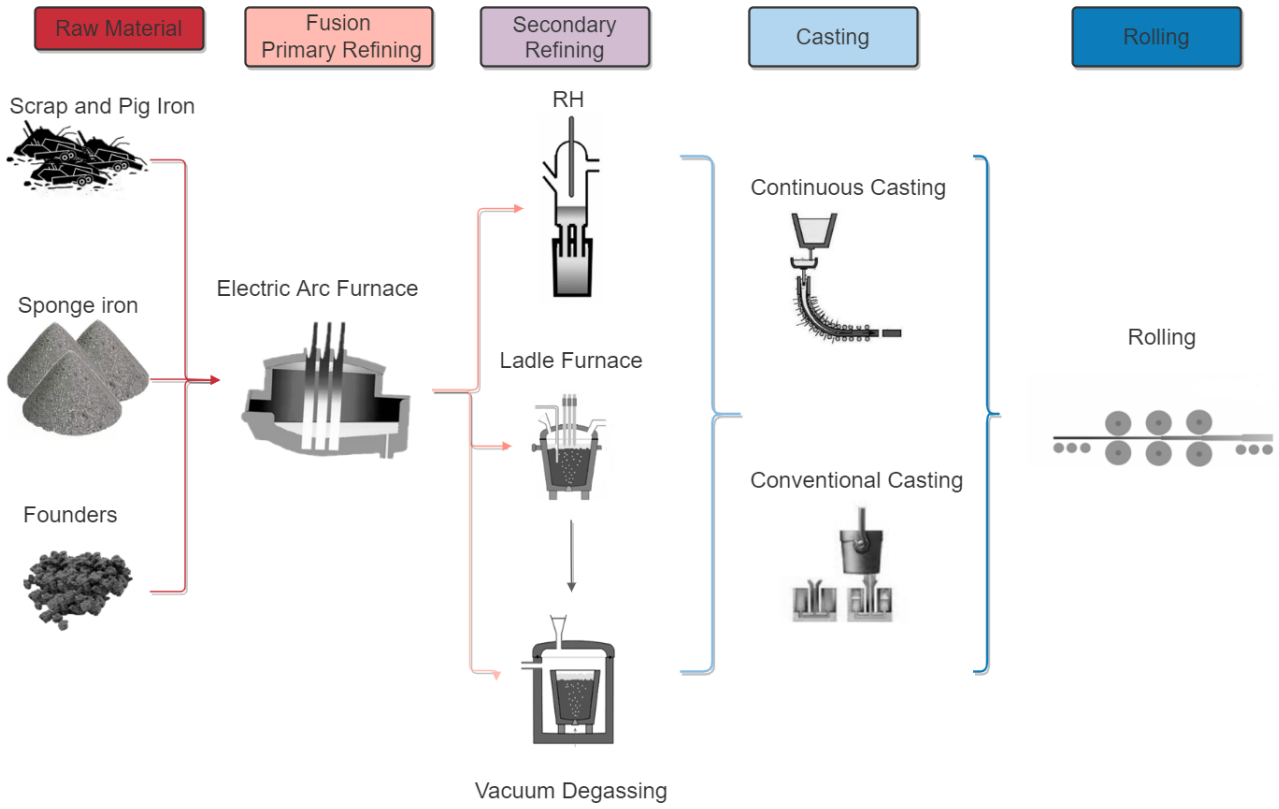

FIGURE 2.5. Flowchart of the steelmaking process stages in an electric secondary steelmaking

2.2.1 Fusion and primary refining

EAFs are used in the steel industry to melt scrap metal at high temperatures, using electric arcs (usually divided into high pressure and low pressure arcs). Graphite electrodes are energy conductors, which are responsible for generating the electric arc that conducts the electric into the material, promoting the melting of the metal charge; these arcs are usually divided into high current and ultra-high current (if the current exceeds 10 kA). Usually oxygen is injected into the molten melt using an oxygen lance; this oxygen, combined with car-

bon, leads to the formation of the slag foaming that acts as a protective layer for the furnace. It is worth noting that many studies show a reduction on energy consummation when increasing the oxygen injection in the bath, because of the exothermic nature of oxidation. During refining, the removal of carbon and other inorganic impurities such as phosphorus, silicon, manganese, aluminum, chromium, etc. are driven by the favored kinetics of the oxygen lances. The oxidized elements are less dense than the liquid metallic phases, float above the and enter the phase slag, which is present above the molten steel. This stage of the steelmaking process is called Primary Refining.

2.2.2 Secondary refining

Secondary refining is characterized as the metallurgical operation of refining and adjusting the chemical composition and temperature of the liquid steel, which is carried out outside the EAF. This in turn is performed through various processes, such as vacuum treatment to remove gases; agitation by gas bubbling to homogenize the bath; the complete mixing of alloying elements; the refining of steel by using synthetic slag; the maintenance of an inert gas atmosphere in the ladle furnace (LF), and even the heating of liquid steel (MACHADO, 2007).

2.2.2.1 Deoxidation

During primary steelmaking, most of the impurities present in the charge (i.e., molten iron, scrap, DRI, etc.) are oxidized and removed. As a result, a large amount of oxygen also remains in the steel in the dissolved state. Dissolved oxygen, if left as it is, seriously impairs mechanical properties of steel and must therefore be removed from the melt before casting.(MAZUMDAR; EVANS, 2010).

Deoxidation or "removal of oxygen" is generally facilitated by the addition of elements like Al, Si, Mn, etc. either individually or in combination, which have larger affinity toward oxygen than iron. Typically, lump additions of deoxidizer elements are made to the bath almost simultaneously with tapping as is illustrated in Figure 2.6.

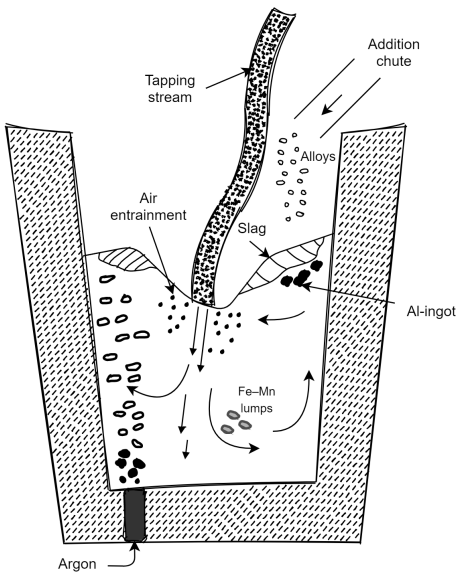

FIGURE 2.6. A schematic of furnace tapping and deoxidizer addition operation.

2.2.2.2 Desulfurization

Desulfurization is an important step in the liquid steel refining process that is done during the inert gas (argon) bubbling, known as rinsing, and aims to reduce the sulfur content in the steel to levels that do not influence the mechanical properties required for each steel grade. This element, in turn, impairs weldability, corrosion resistance, and is responsible for hot embrittlement, which is very harmful to the material's mechanical properties, that is, depending on the application of the steel produced, a high sulfur content has a deleterious effect

on its quality. Besides this, one of the main problems is the appearance of cracks during rolling (ROCHA, 2011; ASTH, 2011; ZANON, 2013).

Equation 2.1 shows one of the main equations for steel desulfurization. Note: "[ ]" refers to molten metal and "( )" to slag.

$$3[S] + 3(CaO) + 2[Al] \longrightarrow 3(CaS) + (Al_2O_3) \tag{2.1}$$

From Equation 2.1 we can conclude the following statements:

- The addition of CaO in the steel bath. Shifts the equilibrium towards the generation of the products and thus calcium sulfide is formed, removing sulfur from the bath and transporting calcium sulfide to the slag.

- The presence of alumina (Al_2O_3) in the slag has the opposite effect. There is a shift of the balance towards the reactions, transferring the sulfur from the slag to the bath.

In the following chapters, we shall comment on methods approached for maximizing steel desulfurization.

2.2.3 Casting

The transformation of liquid steel into a solid product occurs in the casting stage. There are two ways in which this may be accomplished: the traditional method, known as conventional casting, or through continuous casting.

2.2.3.1 Conventional casting

Conventional casting is accomplished by pouring the steel from the ladle, directly or indirectly, into individual molds until it is completely solidified into ingots. This method is simple to operate and requires minimal casting temperature control, and is still used in mills producing specialty steels, or semi-finished steels for the production of flat products (MADRUGA, 2016).

2.2.3.2 Continuous casting

The continuous casting method is carried out through the continuous solidification of liquid steel in a mold with the closest section shape suitable for the mechanical forming process that will generate the final product. Thus, in this process, the liquid steel from the ladle is transferred to a tundish and from there to the molds of the shafts, where the solidification will take place, thus enabling the continuous extraction of billets, blooms, plates or pre-forms (ROCHA, 2014).

According to (RIHL, 2012), the *International Iron and Steel Institute* stated that conventional casting, in 1978, led the steel production chain, accounting for 77.7%, compared to the continuous method, which had not yet gained strength, with only 23.3%. Recently, the *World Steel Association* published a report stating the significant increase in steel production via continuous casting with 96.4% in 2018.

2.3 Slags of secondary refining

By definition, slags of secondary refining are total or partial liquid solutions comprised by oxides and fluorides (usually a mixture of $CaO - MgO -$

$SiO_2 - FeO - Al_2O_3 - CaF_2$) (LUZ et al., 2018). However, these slags are not merely metallurgical waste products but, on the contrary, their compositions and physical properties are judiciously designed to optimize the operations in the respective metallurgical reactors (DIPPENAAR, 2005).

For over half a century, advances have been made in slag research in the United States of America, the United Kingdom, and Germany. In the 1960s, researchers in Japan were already conducting important studies involving measurements and modeling of slag properties (SEETHARAMAN; MUKAI; SICHEN, 2004). Slags are designed to maximize their refining capacity, including optimization of chemical composition as well as physical-chemical properties. The following highlights some of the key functions of secondary refining slags:

- Preventing oxidation of molten steel (ERICSSON; KARASEV; JöNSSON, 2011; PERSSON, 2007; FRUEHAN, 2004);
- Thermal insulation of molten steel (KONONOV; ZEMSKOV, 2012; FRUEHAN, 2004);
- Remove impurities from molten steel (PERSSON, 2007; LIM et al., 2016; FRUEHAN, 2004);
- Remove and modify non-metallic inclusions (SILVA, 2018; REIS; WAGNER; BIELEFELDT, 2013; BIELEFELDT; VILELA, 2014).

Secondary Refining Slag is composed of basic and acidic oxides. Predominantly, in the production of specialty steels, they are composed of CaO, SiO_2, Al_2O_3, and MgO, with lower levels of iron oxides, manganese, and traces of other elements. In the following chapters, slag structures, the chemical composition of slag and the viscosity of slag will be presented in more details.

2.3.1 Slag structures

As previously stated, slags are the remains of minerals (metal oxides, sulfates, etc) generated at high temperature process as byproduct. Within this work, melts are multi-component oxide system and they will have a specific cooling behavior. As a result, the slag may contain a solid fraction cooling, as is illustrated by Figure 2.7 for binary systems.

1. Slag is completely molten at T_{start} above liquidus temperature T_{liq}

2. Cooling below T_{liq} leads to crystallization. A mixture of solid phases (B_{sol}) and liquid (X_{liq}) is formed. The composition of the remaining liquid slag X_{liq} changes when the solidification phase consumes slag components. Under equilibrium conditions, the composition of the remaining slag will change following the liquidus line.

3. Further cooling causes solidification at the eutectic point, X_{liq} = 0. In special cases, when eutectic slag compositions is used, the transformation from liquid to occurs at constant temperature.

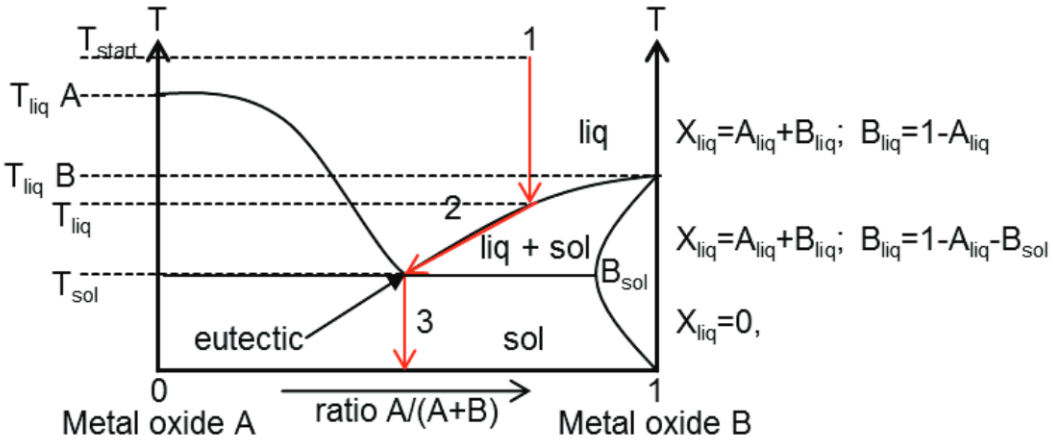

FIGURE 2.7. Schematic of eutectic binary phase diagram of two metal oxides (MEYER et al., 2017)

It is important to point out that below the liquidus temperature slags-systems are in two-phase regions. This work will focus on the representation of the iso-viscosity curves in these conditions as well.

2.3.1.1 Solid Slag Structure

The structure of solidified slags is connected to the structures of glasses. Several structural models were developed, especially for silicates (MEYER et al., 2017).

The basic element for a wide range of structure models is the [SiO_4^{4-}]-tetrahedron or silicate tetrahedron for silicates melts. A silicon atom is positioned in the center of four oxygen atoms bond to the silicon, as in Figure 2.8 illustrated.

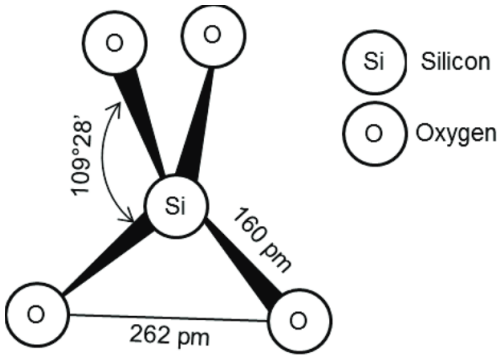

FIGURE 2.8. SiO_4- Tetrahedron

Contrary to the regular symmetrical appearance of tetrahedra within a crystal, the tetrahedra within a glass are occurring in an irregular fashion (Figure 2.9). During cooling, the network of tetrahedra is formed by polymerization.

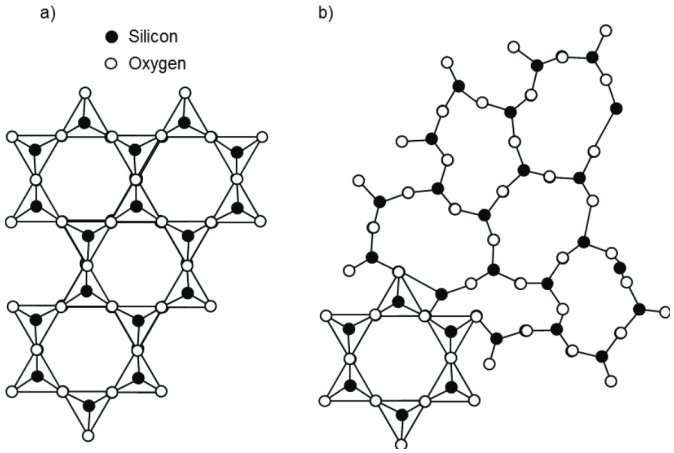

FIGURE 2.9. SiO_4- Tetrahedron connections a) in solid quartz and b) in molten quartz

Below, is provide a list of the network formers found in the literature (DIETZEL, 1942; SUN, 1947; GAO et al., 2014; KIM et al., 2010).

a. Boron
b. Silicon
c. Aluminum
d. Phosphorus
e. Vanadium
f. Titanium

The crystalline or glassy network can be broken by the introduction of other cations in form of metal oxides. The added oxygen will occupy vacant corner of the opened tetrahedron while the large cation enters the hole, thus modifying and weakening the network (Figure 2.10) (KIM et al., 2010; GAO et al., 2014).

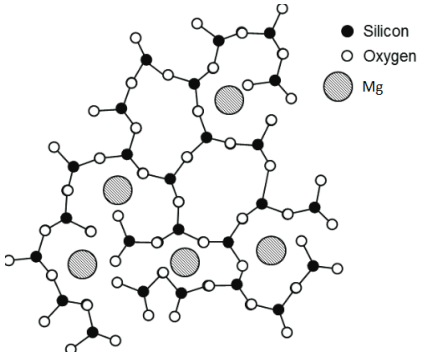

FIGURE 2.10. Weakened glass structure by introduction of MgO as network modifier

Below, it will provide a listing of the network modifiers found in the literature (DIETZEL, 1942; SUN, 1947; GAO et al., 2014; KIM et al., 2010).

a. Lead
b. Magnesium
c. Calcium
d. Sodium
e. Potassium
f. Titanium
g. Aluminum
h. Iron

It is possible to observe that Al presents an amphoteric behavior, because the element presents itself as an network formers and network modifiers. Within a multicomponent slag, amphoteric can either strengthen the tetrahedra network or diminish the tetrahedra network depending on the slag basicity/acidity.

2.3.1.2 Liquid Slag Structure

As pointed out in chapter 2.3.1.1, silicate melts are made of SiO_4^{4-} tetraedra, which joined to form chain of rings by bridging bonding oxygen (BO). Several cations tend to break these structures, such as $Na^+, Ca^{2+}, Mg^{2+}, Fe^+$. These are network modifiers. Non-bring oxygen (NBO) is formed with ions of O^- and free O^{2-}, as Figure 2.11.

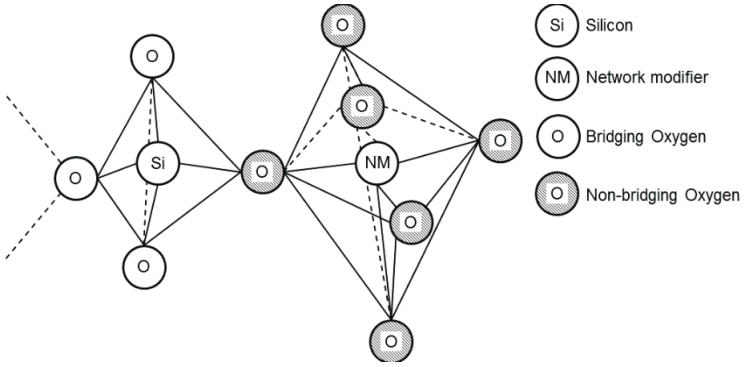

FIGURE 2.11. Schematic representation of tetrahedra formed by Si, O and network modifier

Silicate melts contain various 3-dimension, interconnected anion units such as $SiO_2, Si_2O_5^{2-}, Si_2O_6^{4-}, Si_2O_7^{2-}, SiO_4^{4-}$, which coexist in the melt. The rapid increase of viscosity during the cooling depends on the formation of disordered, infinite networks. Small ionic units with low coordination's number,

such as the [SiO_4] - tetrahedron (coordination number of 4), start polymerization (MEYER et al., 2017).

2.3.2 Chemical composition

The chemical composition of the slag used in Secondary Refining varies considerably depending on the industrial practice of each steelworks. According to the literature, (XU et al., 2014) , calcium-aluminate slags with magnesium represent the basis of most secondary refining slags.Additions of SiO_2 complete the quaternary system guaranteeing very common applications in metallurgical processes. Table 2.1 presents typical composition ranges of slags applied in Secondary Refining based on some references (FUHR et al., 2007; SHAMSUDDIN, 2016; SONG; SHU; SICHEN, 2011; RIYAHIMALAYERI; ÖLUND; SELLEBY, 2013; GUO; CHENG; CHENG, 2014).

TABLE 2.1. Typical chemical compositions of slags in Secondary Refining

Reference	Chemical composition (wt%)						
	CaO	SiO_2	Al_2O_3	MgO	FeO	MnO	S
Fuhr et al.(2007)	50-60	5-15	25-35	5-9	<1.0	<0.2	<0.2
Shamsuddin (2016	50-55	5-12	20-25	9-10	<1.0	<1.0	-
Song, Nzotta e Sichen (2011)	45-56	9-15	23-29	8-21	-	-	-
Riyahimalayeri, Ölund e Selleby (2013)	55-62	6-6.5	29-35	2-5	-	-	0.5-2
Guo, Cheng e Cheng (2014)	53-60	2-2.6	25-36	4-6	-	<0.3	<1

Slags from the quaternary system CaO-SiO_2-Al_2O_3-MgO have great importance when it comes to Secondary Refining of steels, especially with regard to the capture of non-metallic inclusions and refractory protection. It is noted that there is little information available in the literature terms of the phases

present in the equilibrium in these systems, including the composition and proportion of the liquid and solid phases formed (REIS; WAGNER; BIELEFELDT, 2013; BIELEFELDT; VILELA, 2014; BIELEFELDT et al., 2014).

2.3.3 Basicity and B/A-ratio

The ratio between network modifying and network forming ions (also called Basicity) is one of the most utilized and discussed number to describe the properties of slags and glass melts. Moreover, basicity, which is most appropriate to be defined by the activity of free oxygen ions, could be used to monitor free oxygen ions and to understand the equilibrium state of silicate melts (LEE et al., 2008).

Formulations to calculate the basicity, i.e. the B/A - ratio, are given in Equation 2.2 and 2.3, respectively. The amount of components can be introduced as mass fraction, indicated by x (MEYER, 2017).

$$\frac{B}{A} = \frac{Base}{Acid} = \frac{networkmodifiers}{networkformers} \tag{2.2}$$

$$\frac{B}{A} = \frac{x_{CaO}}{x_{SiO_2}} \tag{2.3}$$

In this current work, the following nomenclature will be adopted:

- High basicity slags are slags with B/A >1
- Low basicity slags are slags with B/A <1

2.3.4 Viscosity and thermodynamic models

Viscosity is one of the most important physical properties regarding the refining steelmaking of slags. It may be drastically influenced even by minor changes in the chemical composition and temperature. Optimizing these parameters may affect the reactions between the slag and the liquid steel, promoting relevant phenomena impacting in terms of the steel quality, specifically its cleanliness (PEREIRA et al., 2019; MILLS et al., 2001). The viscous behavior of slags is of great concern to understand its physical-chemical properties, such as gas permeability, heat transfer, the rate of desulphurization and indirectly the rate of FeO reduction, because the presence of MgO favors dissolution of FeO in the steel (PENGCHENG; XIAOJUN, 2016).

The viscosity measurement process is considered expensive, so the cost-effectiveness does not favor the measures at high-temperatures. Alternatively, it is possible to apply mathematical models to obtain viscosities for a given range of chemical composition and temperature of slags (XU et al., 2014). Computational thermochemistry can be used to evaluate the internal structures of the slag and the solid fraction in the system.

The modified *Quasichemical* model (MQM), for example, describes the thermodynamic behavior of the liquid slag in the thermodynamic software *FactSage*. In this software using the *Viscosity* module which used quadruplet data detained from MQM, it is possible to calculate the viscosity of liquid. The MQM model was originally introduced by (PELTON; BLANDER, 1986). The main parameter of the model is the molar *Gibbs* energy of the reaction expressed by Equation 2.4.

$$(A-A)+(B-B)=2(A-B):\Delta g_{AB} \tag{2.4}$$

The MQM theory is based on the balance of chemical reactions of combining oxides with their neighbors present in the slag. Equation 2.4 presents the quasichemical reaction for a binary slag, where the components (A and B) and their particles mix and relocate in the semi-crystalline structure. The thermodynamic properties of ternary solutions can be calculated by interpolating the parameters of the binary model (i.e. Δg_{AB}) in Equation 2.4 (JUNG, 2010). The MQM is flexible and allows for various interpolation techniques and, including, multicomponent slag systems have been successfully modeled using the MQM (JUNG; ENDE, 2020; JUNG, 2010).

In a previous work, viscosity of multicomponent systems were calculated using *FactSage* and compared them to the literature (PEREIRA et al., 2019; ROCHA, 2018). The $CaO - SiO_2 - Al_2O_3 - MgO$ system, in particular, showed an average deviation between the calculated and experimental data of less than 30% overall (CHEN; ZHAO, 2016). It is to be mentioned that, the viscosity of a giving system may show variations of up to 50% between different measuring studies (MILLS et al., 2001).

Complementing previous papers (PEREIRA et al., 2019), the current work aims to calculate the viscosities of different sets of chemical composition, for slags of the CaO-SiO_2-Al_2O_3-MgO system, for different temperatures, and for partially liquid, (two-phase) slags.

2.3.5 Slag Components

As pointed out in Chapter 2.3.1.1, oxide components are modulation the structure and therefore the physico-chemical properties of slags. A summary and short overview of different oxide components is given in the following sections.

2.3.5.1 Silicon dioxide

Silicon oxide plays the most important role in the slag viscosity behavior. The chemical and structural behavior of SiO_2 was introduced in detailed in Chapter 2.3.1.1. As a network former, it increase the viscosity of slags.

2.3.5.2 Aluminum oxide

Alumina, Al_2O_3, is known to be an amphoteric oxide it behaves either as a basic oxide and a network modifier or an acidic oxide and a network former depending on the overall slag composition. A decrease in the network-modifying component can polymerize the slag structure and increase the viscous behavior of the slag. Considering that, Al_2O_3 additions increased the viscosity, Al_2O_3 likely polymerized the slag structure and behaved as a network forming acidic oxide (ZHANG; CHOU, 2013; KIM et al., 2013; WANG et al., 2020).

Figure 2.12 shows the effect of Al_2O_3 additions at a constant temperature of 1773K (1500ºC) (KIM et al., 2013).

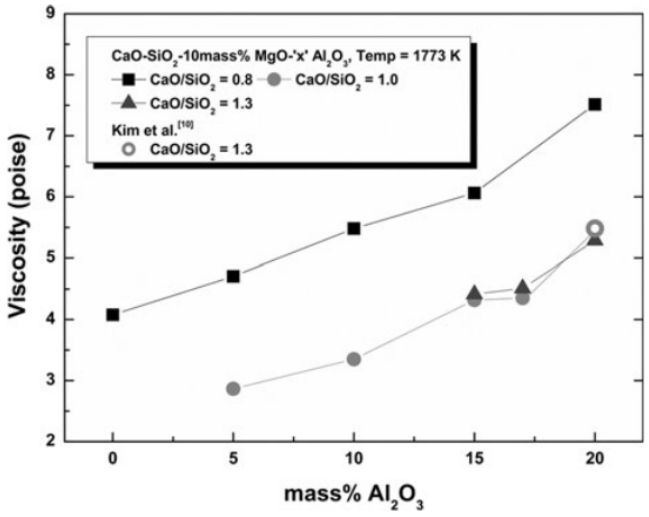

FIGURE 2.12. Effect of Al_2O_3 on the viscosity of the calcium-base slags containing 10wt.%. MgO at 1773 K (1500°C) - [10 poise - 1Pa.S]

The increase in viscosity with Al_2O_3 addition at 1773K seems to be independent of the basicity (between 0.8 to 1.3). At a constant wt.% of Al_2O_3, an increases in the basicity from 0.8 to 1.0 decreases the viscosity of the slag. The effect of increasing the basicity from 1.0 to 1.3 seems to be negligible within the current slag system.

The effect of varying the CaO/SiO_2 at fixed Al_2O_3 of 15 and 20wt.% for different temperatures of 1698K and 1773K is shown in Figure 2.13 (KIM et al., 2013).

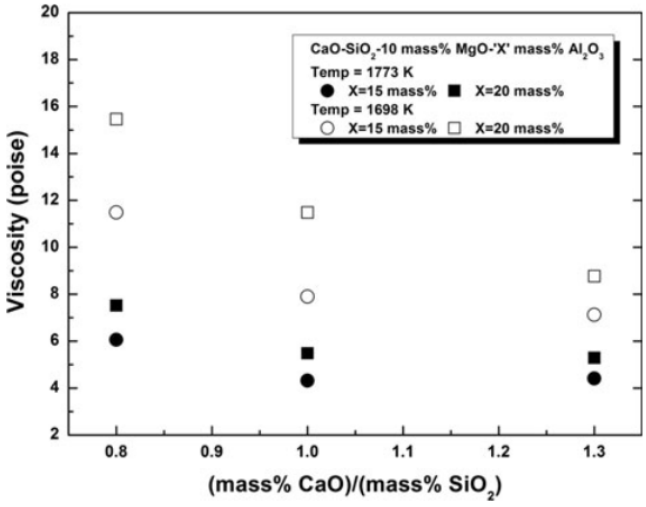

FIGURE 2.13. Effect of the CaO/SiO_2 ratio on the viscosity of calcium-alumino-silicate-based slags containing 10wt%. MgO at 1698K and 1773K with 15wt%. and 20wt%. of Al_2O_3

At 1698 K, an increase in the basicity of 0.8 and 1.0 leads to an appreciable decreases in viscosity; a subsequent increase in the basicity from 1.0 and 1.3 has almost no effect on the viscosity. At 1773K, an increase of the basicity from 0.8 to 1.0 slightly lowers the viscosity. Subsequent increase in the basicity from 1.0 to 1.3 has virtually no impact on the viscosity.

2.3.5.3 Calcium oxide

Calcium oxide, CaO, is an alkaline earth oxide and is defined as a network modifier. CaO is donates oxygen ions and therefore opens the silicate network, which lowers the viscosity. The literature presents several studies of the effect of CaO on the viscosity of slags. Work that studied a slag with a high concentration of titanium oxide to visualize the effect of CaO/SiO_2 (FENG et al., 2019) is presented next.

This work explored viscous behaviors of $CaO - SiO_2 - 11{,}00wt,\%MgO - 11{,}00w\%tAl_2O_3 - 43{,}00wt,\%TiO_2$ slag systems the study determined the effects of CaO/SiO_2 ratio on the viscosity of various slags as shown in Figure 2.14.

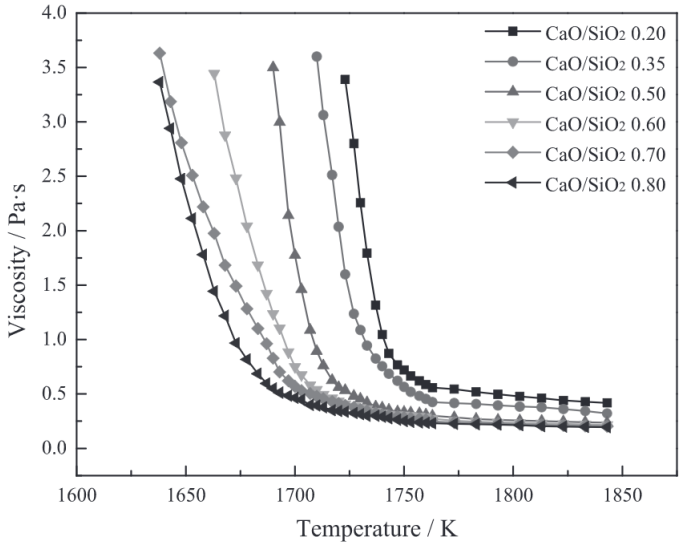

FIGURE 2.14. η-T of different CaO/SiO_2 experimental titanium-bearing slags

It is clear from the Figure 2.14 that the viscosity of slags increases when the temperature is lowered. There exists a breaking point in temperature (temperature which there is no change in viscosity) foreach η-T curve. When the temperature is higher than the breaking point temperature, the variation of the viscosity as a function of temperature is small, and fluidity and the thermostability of the slag is good as well in this temperature range (FENG et al., 2019). Above the breaking point the temperature of slags viscosity decreases as the CaO/SiO_2 ratio is increased. As CaO/SiO_2 ratio increases, the availability of free oxygen regions (O^{2-}) in the molten slag increases as well CaO dissociations. These provided O^{2-} can react with the O^0 in the network structure to form the non-bridging oxygen (O^-), and the complex networks are depolymerized to the small units, such as monomers. Thus, the viscosity of the experi-

mental slags decreases with increasing CaO/SiO_2, and the fluidity is improved (FENG et al., 2019).

2.3.5.4 Magnesium oxide

Magnesia, or MgO, is defined as a network modifier (CHEN; HE, 2015; PENGCHENG; XIAOJUN, 2016). It also reduces the slag viscosity but to a lesser extant than CaO. A general network modifying behavior was found by (PENGCHENG; XIAOJUN, 2016) for $CaO - MgO - SiO_2 - Al_2O_3$ for different temperatures. Figure 2.15 shows the decrease of viscosity when increasing the MgO content of different slags.

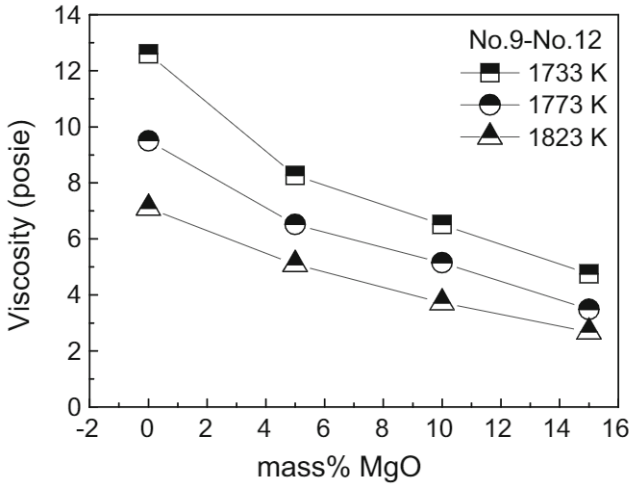

FIGURE 2.15. Effect of MgO on viscosity of $CaO - MgO - SiO_2 - Al_2O_3$ slags

2.4 Computational thermodynamics - *FactSage*

The search for alternative technologies to obtain "clean" steels with excellent mechanical properties has led the specialty steel industry to invest in

research and technology. Computer simulations show great strength in understanding many industrial processes. One of the well-known simulation tools is computational thermodynamics.

Thermodynamic simulations have been used to understand many phenomena that occur during the processing of liquid steel, for which a large number of reactions may occur. The application of computational thermodynamics facilitates the resolution of problems previously addressed with tabulated data and an equilibrium diagram.

In addition, (JUNG; ENDE, 2020) reports, in detail, an overview of a computational thermodynamics software, *FactSage*. In addition, it presents the modules and packages available in the area of computational thermodynamics.

FactSage is a commercially available software which was introduced by Pelton and Bale (BALE et al., 2016), During these two decades the software has received several updates on its databases, interface and modules (JUNG; ENDE, 2020; BALE et al., 2016; GHERIBI et al., 2012; JUNG, 2010).

Because of its extensive databases, *FactSage* is capable of calculating phase diagrams and phase equilibrium conditions for multi-component systems. The software's database contains information about the thermodynamic behavior of many individual phases as well densities, and liquid viscosities as a function of temperature, pressure, and composition (GHERIBI et al., 2012). The knowledge of thermodynamics becomes useful when performing process simulations, many modules available in the software (ROCHA, 2016).

In this work, two major modules were used, the *Equilib* and *Viscosity* modules. The *Equilib* module was used with the following databases: *FactPS* and *FToxid*. We used, the *Viscosity* module with the Melts database. Further details of these two modules will be presented below:

- Data base selection in Equilib:
  - FactPS: This database contains thermodynamic data of over 4900 stoichiometric solid, liquid, gas and ions compounds.
  - FToxid: The FACT oxide database (FToxid) contains thermodynamic parameters for pure oxides and oxide solid solutions formed by 23 elements (as well as for dilute solutions of $S, SO_4, PO_4, H_2O/OH, CO_3, F, Cl$ and I in the molten slag phase) obtained from a critical assessment of the avaible experimental data in the literature.
- Viscosity
  - Melts: liquid and supercooled slags with viscosities which are not too high ln(viscosity, Pa·S) < 15

Computational thermodynamics applied to solid steel, liquid steel, slag and solid oxide solutions of various system components has been developed over the past three decades through a critical assessment process and evolution of the thermodynamic optimization (JUNG; ENDE, 2020). The evolution of the thermodynamic modeling is happening at the same pace as the improvement of machine performance and processing capacity. Within the steel industry environment, *FactSage* has many applications. Among them, research related to the following phenomena stand out:

- Alkali Circulation and Corrosion of Refractoryin Blast Furnace
- Heat Balance in the Alloying Process
- Degassing Process
- Deoxidation Equilibria in High Mn Steel

- BOF Process: De-phosphorization of Hot Metal
- Reoxidation During Casting
- Solidification of Mold Flux
- Casting of Steel: Scheil Cooling Calculation

Chapter 3

Methodology

The methodology adopted in this study is presented in this section. This chapter is divided into the presentation of a general flowchart involving the various steps of the calculation of slag viscosities and the details of the collection of slag viscosity experimental results. Finally, calculations and other information applied in this study are presented.

Figure 3.1 illustrates, in a schematic way, the flow chart of the adopted computational process.

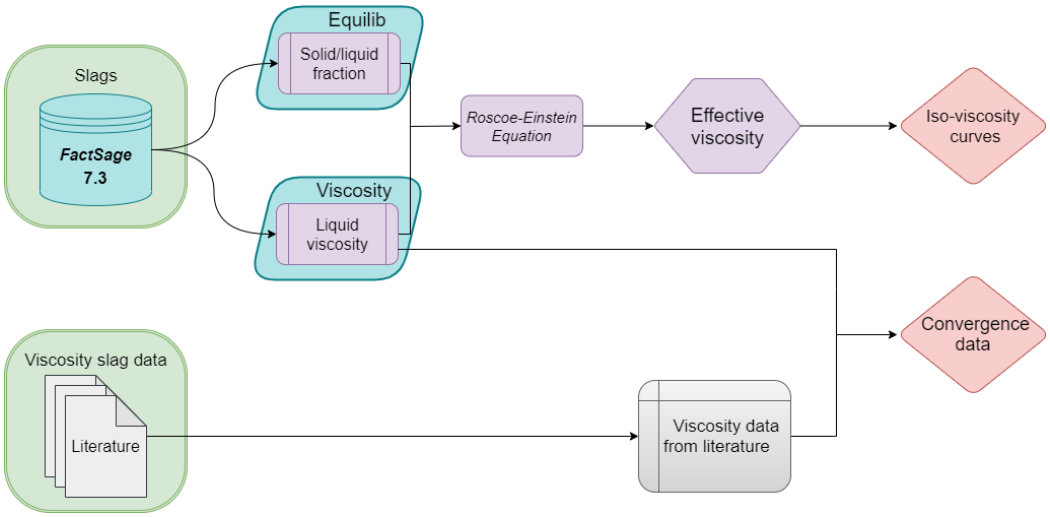

FIGURE 3.1. Flow chart of the computational process in this work.

According to the computational procedure (Figure 3.1), is divided in two parts. The first part consists of performing viscosity calculations using the *FactSage* software and with the *Roscoe-Einstein* equation to perform calculations of the effective viscosity in multiphasic system in which the slag phase contains various fractions of solids.

In the second part, in the second front, a collection of slag viscosity data from secondary refining are collected from the literature references to evaluate the performance of *FactSage* in predicting the slag viscosity of different multicomponent system.

3.1 Thermodynamic computations

The computational thermodynamics technique was applied in this work using the commercially available *FactSage* software, version 7.3. The databases employed in this study were two, (1) *FactPS* (for stoichiometric pure substances) and (2) *FToxid* (for oxides). Both databases were useful in the creation of ternary diagrams and slag viscosity calculations. Figure 3.2 illustrates the main screen of the *FactSage* 7.3 software.

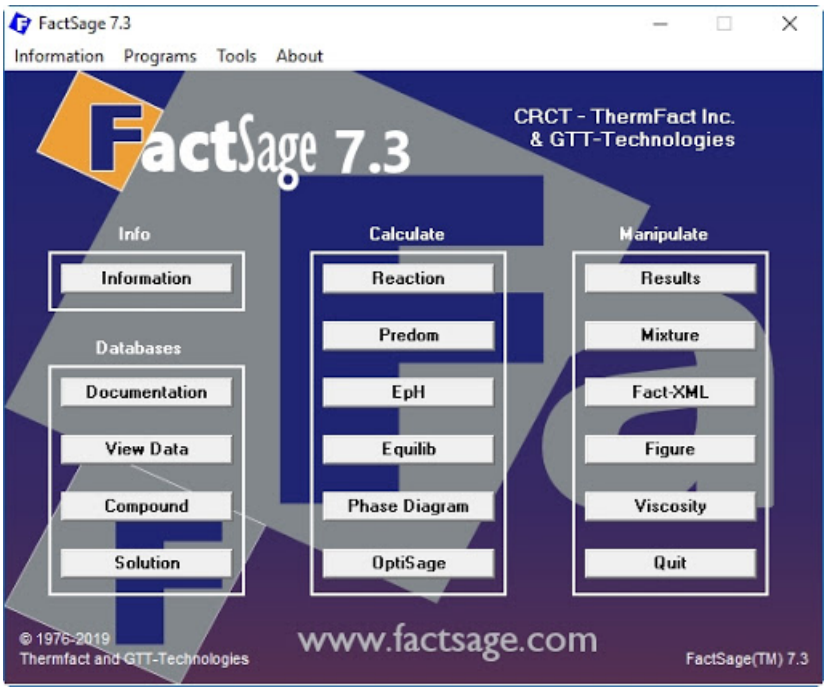

FIGURE 3.2. Main screen of FactSage 7.3

The modules employed in this study were (1) the *Equilib* module for obtaining the liquid fraction and respective chemical composition of the slag, (2) the *Viscosity* module for liquid viscosity calculations. Currently, *FactSage* is of the 8 version, with database revisions and updates from previous versions (JUNG; ENDE, 2020).

The thermodynamic calculations in this work, were performed using 7.3 version.

3.1.1 Solid/liquid fraction of slag

The *Equilib* module allows, through the selected databases (i.e. *FactPS*, *FToxid*) to obtain the solid/liquid fraction and the respective chemical composi-

tion of the phases in equilibrium. To do this, simply feed the module with the overall chemical composition of the system (CaO, SiO_2,Al_2O_3, MgO). (REIS; WAGNER; BIELEFELDT, 2013) described in detail the *Equilib* module menu including the selected systems as well as the obtained results fractions formed (liquid and solid).

The chemical composition of the liquid phase, resulting from the *Equilib* module, is then used as an input data for the calculation of the viscosity in the *Viscosity* module.

3.1.2 Effective viscosity of the slag- η

In the Viscosity module, the viscosity of single-phase liquid slag can be calculated, that is, without considering the presence of solids. Thus, the viscosity calculation can not estimate the viscosity of Secondary Refining slags, since there is typically the presence of solid fraction. To estimate the viscosity when some solid fractions is present, the following equation proposed in 1952 by Roscoe-Einstein (ROSCOE, 1952) was adopted.

$$\eta = \eta_l(1 - \rho f)^{(-2,5)} \tag{3.1}$$

In Equation 3.1, η_l represents the viscosity of the liquid and f the solid fraction, both obtained via *FactSage* with the *Equilib* module. The literature presents a brief script for using *FactSage* 6.4 for liquid viscosity calculations (ROCHA, 2014). The factor ρ represents a solid interaction parameter that, in this study, considering a dilute concentration of spherical particles of different sizes, is assumed to be equal to 1 (BIELEFELDT et al., 2014). The value of the exponent in Equation 3.1 is associated with the geometric shape of the solid particle (ROSCOE, 1952). The application of Equation 3.1 is limited to the assump-

tion that solid particles with low solubility in the liquid slag are homogeneously distributed (SEOK, 2007).

3.2 Literature vs FactSage viscosity calculations

In order to verify the accuracy of the *FactSage* 7.3 software in evaluating the viscosity in the CSAM system, experimental viscosity data were collected through several published works (MACHIN; HANNA, 1945; MACHIN; YEE, 1948; MACHIN; YEE; HANNA, 1952; MACHIN; YEE, 1954; KOZAKEVITCH, 1954; KOZAKEVITCH, 1960; KOZAKEVITCH; MISRA, 1966; J.; M, 1995; SAITO et al., 2003; KIM et al., 2010; SONG; SHU; SICHEN, 2011; CHOPRA; TANEJA, 1964; URBAIN; BOTTINGA; RICHET, 1982; TANG et al., 2011; SHANKAR, 2007; FORSBACKA et al., 2007; GAO et al., 2014; SCHUMACHER; WHITE; DOWNEY, 2015). In these works, the viscosity data were obtained by different methods. Table 3.1 shows more detailed information about the experiments in the viscosity measurement from the literature adopted in this work and the number of the data collected data.

The composition ranges of all the reference source data, are presented in Table 3.2.

The composition ranges, at 1500°C, of some reference source, i.e. (MACHIN; HANNA, 1945; MACHIN; YEE, 1948; MACHIN; YEE; HANNA, 1952; MACHIN; YEE, 1954; KOZAKEVITCH, 1954; KOZAKEVITCH, 1960; KOZAKEVITCH; MISRA, 1966; J.; M, 1995; SAITO et al., 2003; KIM et al., 2010; SONG; SHU; SICHEN, 2011), data are illustrated in pseudo ternary systems presented in Figure 3.3.

TABLE 3.1. Reference sources of the experimental viscosity data.

System	Author	Method	Crucible	Data
	Machin,1945	Oscillating	Pt	5
	Machin,1948	Oscillating	Pt	43
	Machin,1952	Oscillating	Pt	16
	Machin,1954	Oscillating	Pt	12
	Kozakevitch,1954	Rotating cylinder	Mo/W	12
CaO–SiO_2–Al_2O_3	Chopra et al,1964	-	-	14
Data:138	Urbain,1982	Rotating cylinder	Mo	28
	Pengcheng, 2016	Rotating cylinder	Mo	8
	Machin,1945	Oscillating	Pt	15
	Machin,1952	Oscillating	Pt	48
	Machin,1954	Oscillating	Pt	32
	Hoffman,1959	-	-	10
	Kozakevitch,1966	Rotating cylinder	Mo/W	3
	Kowalski,1995	-	-	27
	Tang,2001	Rotating cylinder		84
CaO–SiO_2–Al_2O_3–MgO	Saito,2003	Rotating cylinder	Pt/Rh	3
Data: 432	Shankar,2007	Rotating cylinder		30
	Forsbacka,2007	Rotating cylinder	Cr/Mo	70
	Kim,2010	Rotating cylinder	Pt/Rh	4
	Song,2011	Rotating cylinder	Mo	6
	GaO Y,2014	Rotating cylinder	Pt	24
	Schumacher,2015	Rotating cylinder	Graphite/Mo	25
	Pengcheng, 2016	Rotating cylinder	Mo	51
Total Data				**570**

TABLE 3.2. Composition ranges of slags of the reference sources by %mass.

System	Temperature (°C)	MgO	SiO_2	Al_2O_3	CaO
SiO_2–Al_2O_3–CaO	1400-2083	0	0 - 70	0 - 54	10 - 55
SiO_2-Al_2O_3–CaO–MgO	1372-1720	0 -38	10 - 65	0 - 30	1.5 - 55

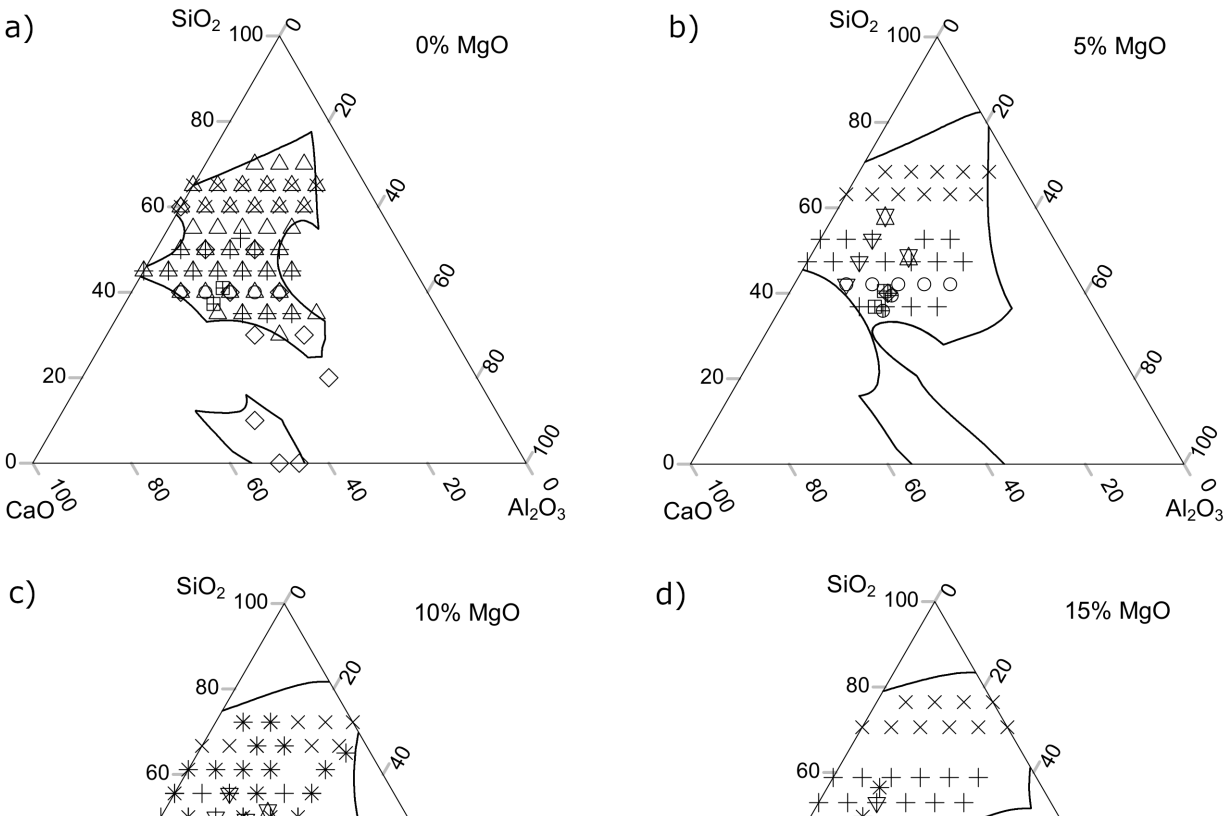

Finally some experimental data at 1500°C used in the present work are presented in Figure 3.3. For each reference, a different symbol was adopted.

To quality the error between the *FactSage* calculations ($\eta_{Calculated}$) and the reference viscosity data ($\eta_{Reference}$), for each slag composition, the Percent Error was calculated using the following expression:

$$\delta_i = \frac{\eta_{Calculated} - \eta_{Reference}}{\eta_{Reference}} \times 100\% \tag{3.2}$$

The average performance analysis of the reference source on viscosity (η) calculations through *FactSage* was evaluated by the Average Percent error, Δ, for N measurements of viscosity, using Equation 3.3.

$$\Delta = \frac{1}{N} \sum_{i=1}^{N} \delta_i \times 100\% \tag{3.3}$$

3.3 Iso-viscosity curves

The thermodinamic simulations were carried out through the Equilib and *Viscosity* modules, both available in *FactSage* 7.3. In the *Equilib* module, the databases used were *FactPS* (stoichiometric pure substances) and *FToxid* (for oxides and sulfur) in order to obtain values for the solid fraction of slags. The Viscosity module uses *Melts* databases and provides the apparent viscosity (η_l). The Roscoe-Einstein (ROSCOE, 1952) equation was used to calculate the effective viscosity (η) of multiphasic system according to Equation 3.1.

Table 3.3 shows the chemical composition range for each slag system used in the viscosity calculations for the creation of iso-viscosity curves.

TABLE 3.3. Composition ranges, in wt.%. , of calculated slags in the viscosity database.

					CaO		SiO_2		Al_2O_3		**count**
					min	**max**	**min**	**max**	**min**	**max**	
Temp	MgO	**Phase Mixture**	**Liquid Phase**	**Solid Phase**							
1500	**0**	×			0	98	0	98	0	98	739
			×		0	60	0	100	0	80	553
				×	0	100	0	34	0	100	34
	5	×			0	93,1	0	95	0	93,1	792
			×		0	53,2	0	89,3	0	58,9	503
				×	0	95	0	34,2	0	95	31
	10	×			0	88,2	0	90	0	88,2	902
			×		0	46,8	0	84,6	0	52,2	394
				×	0	90	0	36	0	90	30
	15	×			0	83,3	0	85	0	83,3	925
			×		0	44,2	32,3	81,6	0	35,7	371
				×	0	85	0	35,7	0	85	29
1600	**0**	×			0	98	0	96	0	98	545
			×		0	60	0	100	0	82	749
				×	0	100	0	34	0	100	32
	5	×			0	93,1	0	95	0	93,1	596
			×		0	57	0	91,2	0	66,5	702
				×	0	95	0	34,2	0	95	28
	10	×			0	88,2	0	90	0	88,2	736
			×		0	48,6	0	88,2	0	57,6	566
				×	0	90	0	32,4	0	90	24
	15	×			0	83,3	0	74,8	0	83,3	853
			×		0	44,2	27,2	85	0	45,9	453
				×	0	85	0	30,6	0	85	20
1700	**0**	×			0	98	0	80	0	98	441
			×		0	62	0	100	0	84	853
				×	0	100	0	34	0	100	32
	5	×			0	93,1	0	95	0	93,1	437
			×		0	58,9	0	93,1	0	74,1	867
				×	0	95	0	34,2	0	95	22
	10	×			0	88,2	0	84,6	0	88,2	545
			×		0	50,4	0	90	0	61,2	761
				×	0	90	0	32,4	0	90	20
	15	×			0	83,3	0	74,8	0	83,3	713
			×		0	45,9	0	85	0	57,8	593
				×	0	85	0	30,6	0	85	20
Total											15911

Each chemical composition is associated to a specific viscosity. The chemical compositions adopted in this work covered all the single-phase liquid re-

gions and some 2-phase regions. The spacing between each composition is in the order of 2wt.%. This variation is related to the size of the stability phase region. A total of 15910 compositions were used to generate production of the iso-viscosity curves.

All iso-viscosity curves were created using an open source software in *Python* (ROSSUM; JR, 1995). The iso-viscosity curves were generated by linear interpolation of the viscosity of the slag.

Chapter 4

Results and discussion

This chapter covers all the results obtained based on the objectives listed at the beginning of this study (see Chapter 1). Each result is discussed in order to debate important foundations described in the literature. The topics in this chapter are divided into two parts, first the convergence of the data calculated via *FactSage* and the data collected by the literature references will be presented. Secondly, the influence of the temperature on the slag viscosities will be introduced, then the influence of the oxides on the chemical composition of the slag and finally the influence of the solid/liquid fraction of the slag. The representations of iso-viscosity curves served as support for the generation of these discussions.

4.1 Precision of the viscosity model available in *FactSage*

The comparison the between experimental viscosity data (from the reference data presented in Table 3.1) and the calculated viscosities, by *FactSage*, is illustrated in Figures 4.1.

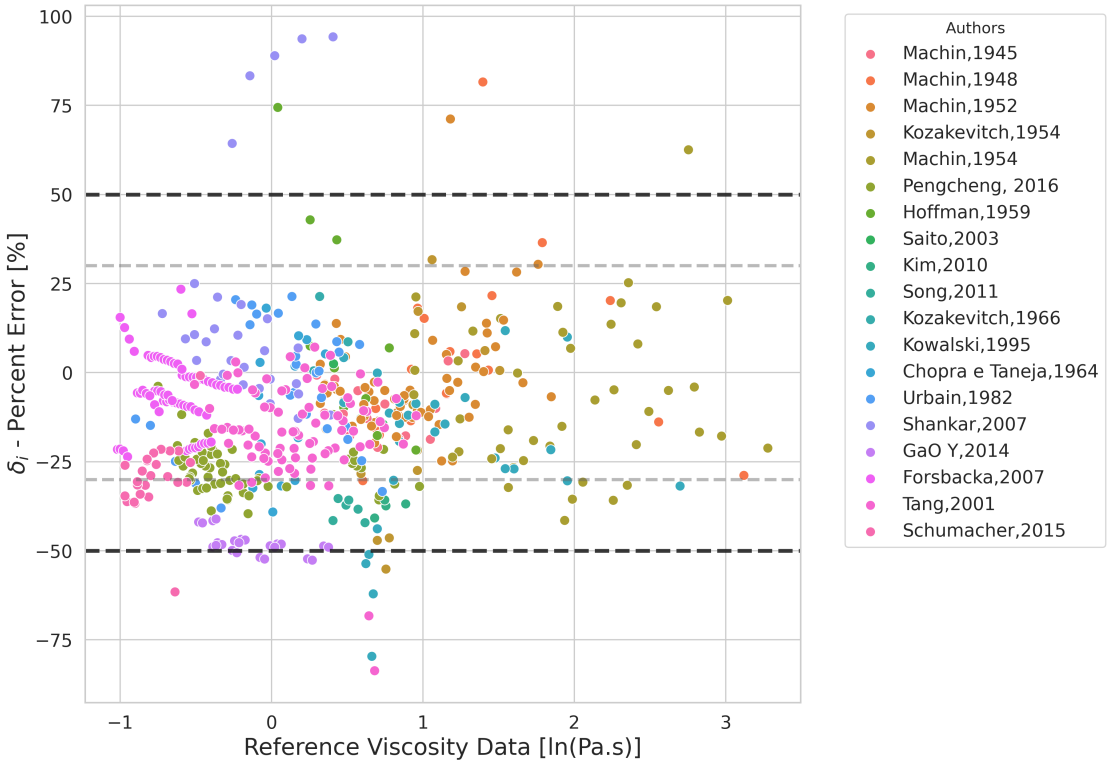

FIGURE 4.1. Percentage error and measured ln viscosity

Regarding the comparative analysis shown in Figure 4.1, the possibility of errors and uncertainties in the experimental data will be taken into account by up to 30%, as proposed by (SUZUKI; JAK, 2013; MILLS et al., 2001; ROCHA, 2014).

Figure 4.2 shows the average relative error as calculated using Equation 3.3. The average relative error between the measured and calculated viscosities is about 20%. In some cases, it is possible to see a more significant error of up to 30%, in the case of as shown in Figure 4.2.

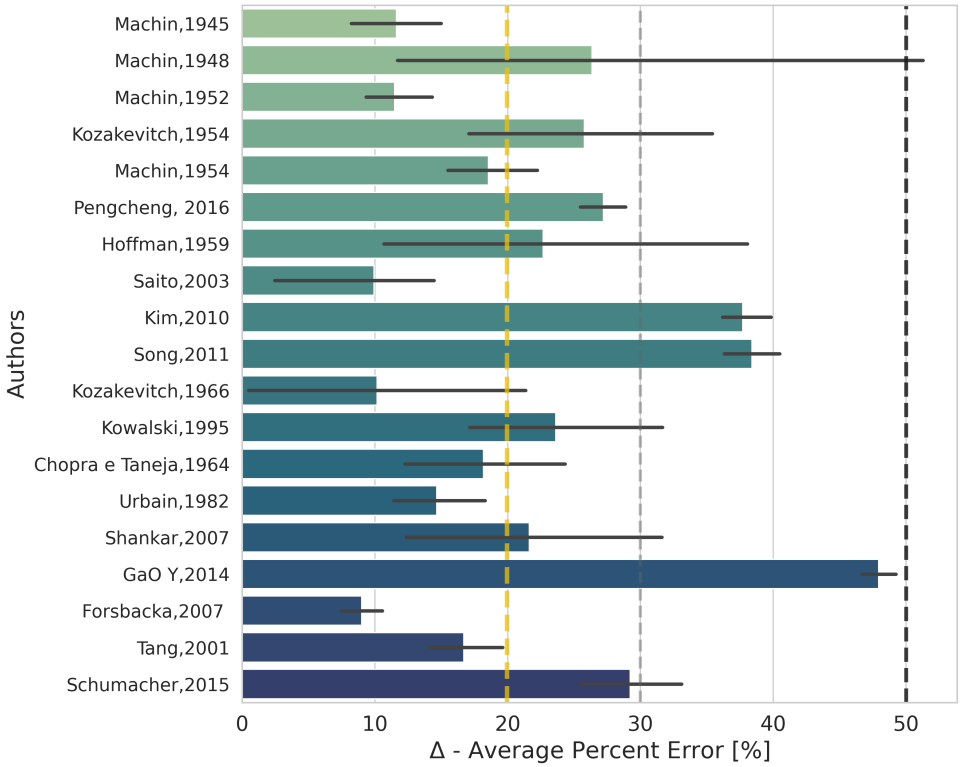

FIGURE 4.2. Average relative error between calculated from FactSage 7.3 and measured viscosity comparison for each reference.

According to (MILLS et al., 2001), the viscosity measurements were subject to experimental uncertainties, such as temperature differences between the thermocouple reading and the actual temperature of the melt. Because of this, viscosity measurements differ from recommended values by an average of ± 30%, and in some cases, more than 50% (KIM et al., 2013; SONG; SHU; SICHEN, 2011; GAO et al., 2014). In this context, it can be said that the obtained results in terms of relative deviation validate the quality of the viscosity model implemented in *FactSage*.

4.2 Slag behavior

In this section we evaluate the viscosity behavior of the slag, in terms of its chemical composition, liquid/solid fraction, and temperature.

4.2.1 Influence of slag composition

It will discussed and visualized the effect of chemical composition of the slag in relation to the liquid/solid fraction of the slag and the viscosity of the slag.

4.2.1.1 Effect the composition on the slag viscosity

The effect of the chemical composition on different combinations of oxides at 1500, 1600 and 1700°C on the viscosity, expressed in ln(Pa.s), can be visualized in Figures 4.3, 4.4 and 4.5. The i.e. figures show a viscosity scale in red coloration, the slags that show the most red coloration are more viscous, and on the other hand the slags with lower viscosities is shown in white coloration.

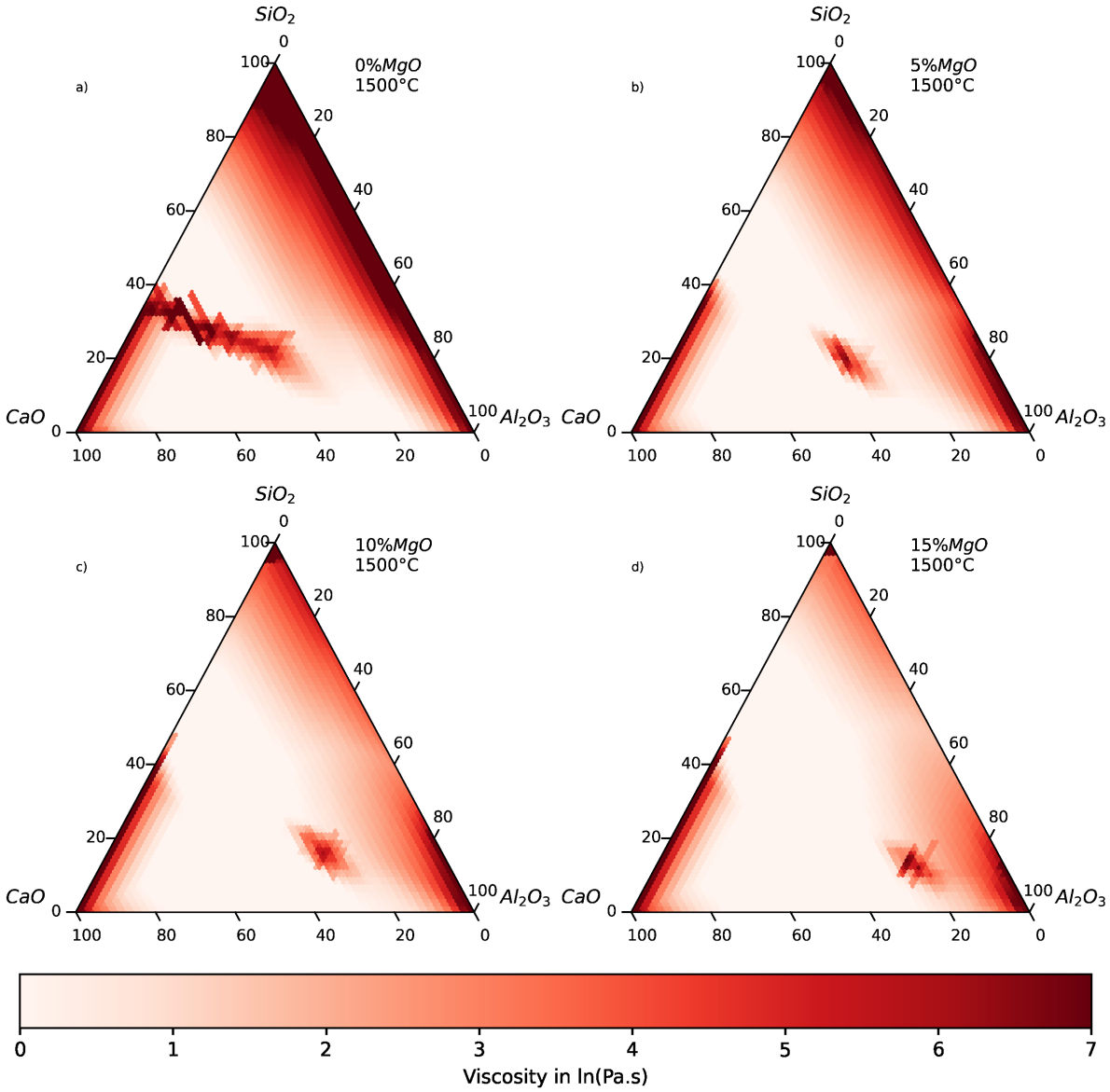

FIGURE 4.3. Iso-viscosity ln([Pa.s]) curves of slags in Liquid and Two-Phase regions: (a) CaO-SiO_2-Al_2O_3 system (wt.%); (b) normalized CaO-SiO_2-Al_2O_3–(5%MgO) system (wt.%); (c) normalized CaO-SiO_2-Al_2O_3–(10%MgO) system (wt.%); and (d) normalized CaO - SiO_2 - Al_2O_3–(15%MgO) (wt.%), at 1500°C.

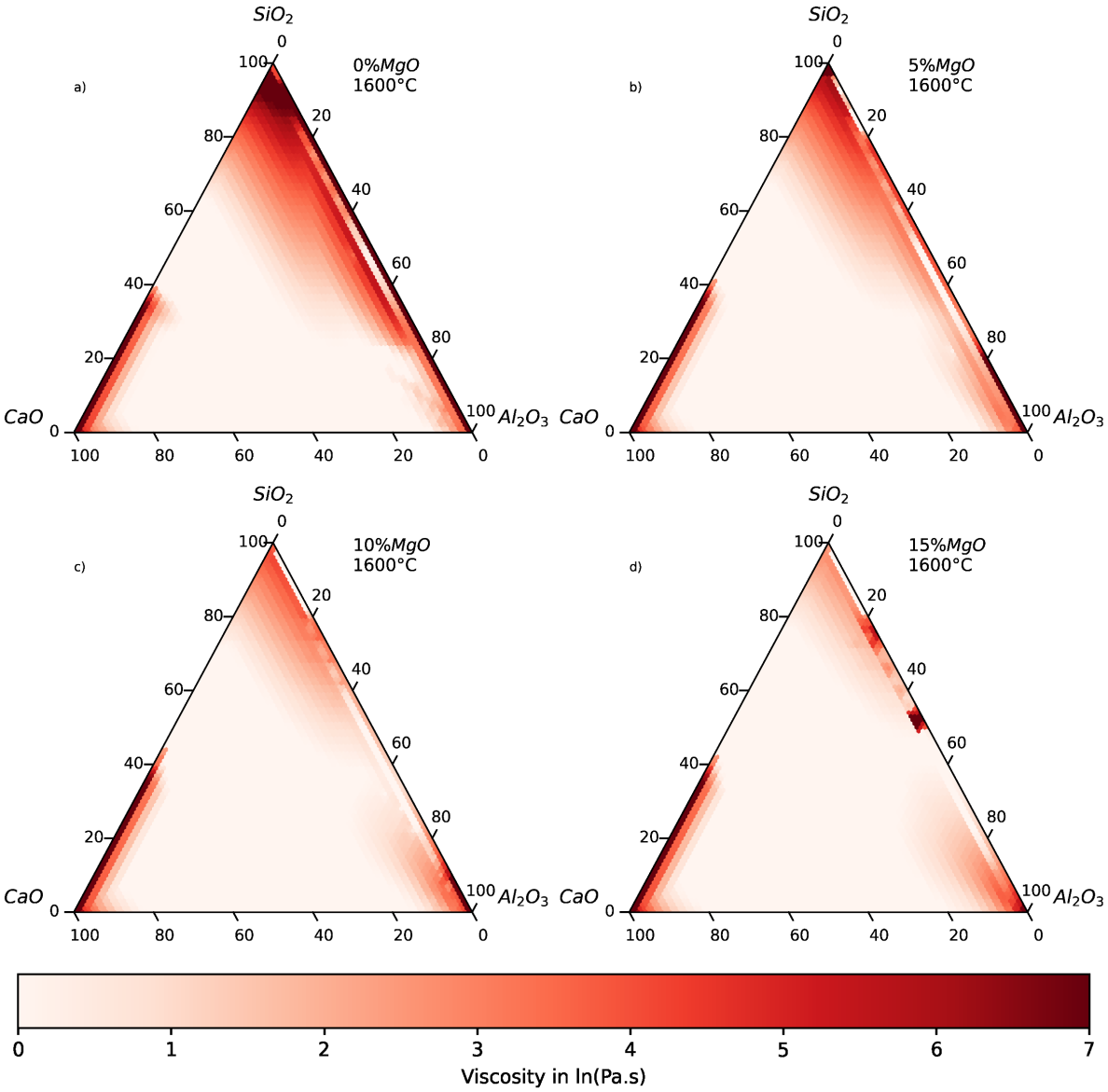

FIGURE 4.4. Iso-viscosity ln([Pa.s]) curves of slags in Liquid and Two-Phase regions: (a) CaO-SiO_2-Al_2O_3 system (wt.%); (b) normalized CaO-SiO_2-Al_2O_3–(5%MgO) system (wt.%); (c) normalized CaO-SiO_2-Al_2O_3–(10%MgO) system (wt.%); and (d) normalized CaO - SiO_2 - Al_2O_3–(15%MgO) (wt.%), at 1600°C.

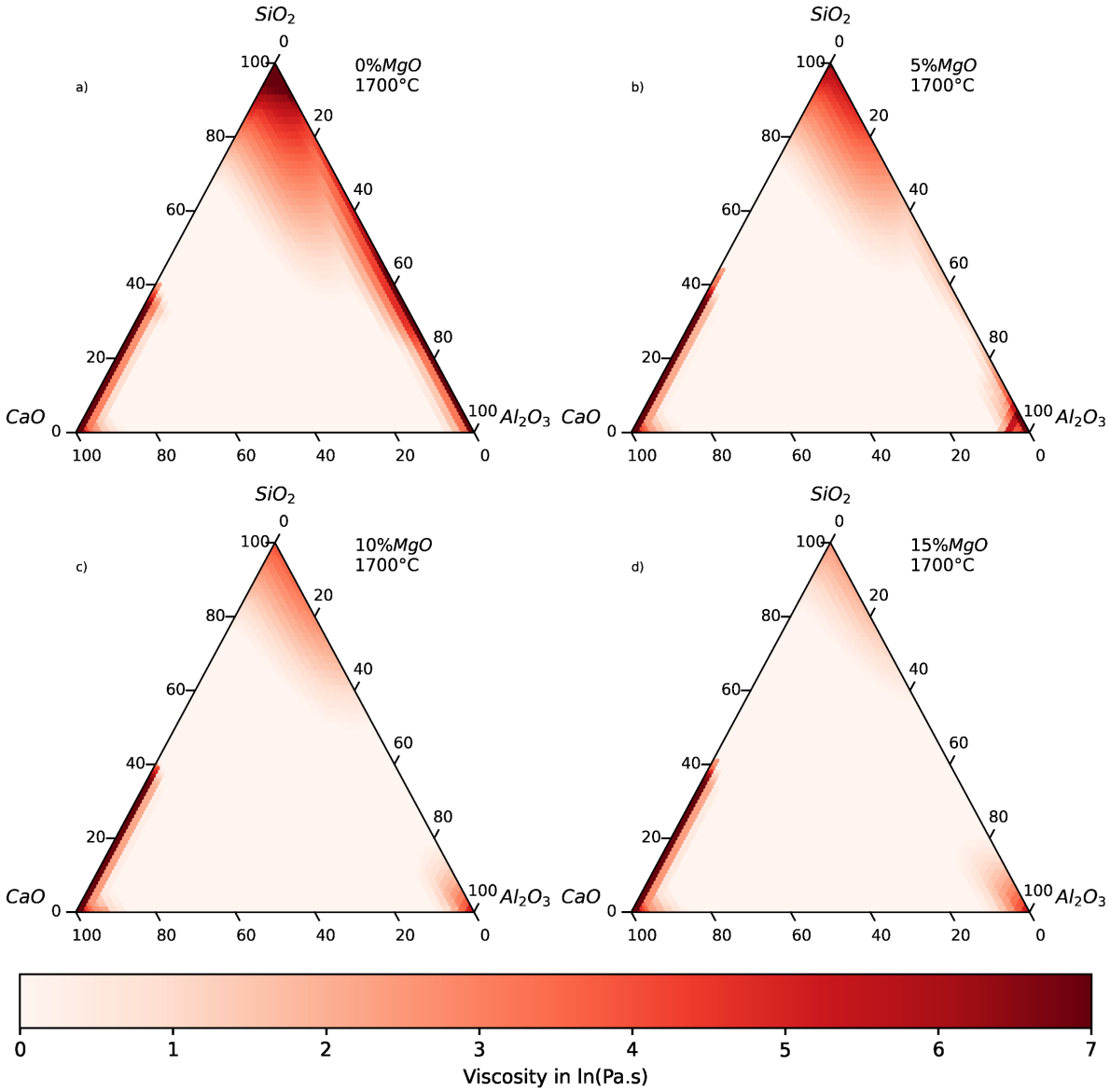

FIGURE 4.5. Iso-viscosity ln([Pa.s]) curves of slags in Liquid and Two-Phase regions: (a) CaO-SiO_2-Al_2O_3 system (wt.%); (b) normalized CaO-SiO_2-Al_2O_3–(5%MgO) system (wt.%); (c) normalized CaO-SiO_2-Al_2O_3–(10%MgO) system (wt.%); and (d) normalized CaO - SiO_2 - Al_2O_3–(15%MgO) (wt.%), at 1700°C.

The impact of each oxide component on the slag viscosity is presented

below:

CaO showed an impact on the viscosity of slags as described in the literature. An increase in CaO content lowers the viscosity of the melt. Significant viscosity decreases were found for low C/S wt.ratios (<1). Higher amounts of CaO are less effective at reducing the melt viscosities (MEYER, 2017). This effect can be explained because, as long the silicate network is not too much depolymerized, the network modifying behavior is still effective. In C/S wt.ratios highers than 1 the slag has reached the breaking point so the addition of CaO does not show a noticeable reduction in viscosity.

The increase of the SiO_2 content in the molten slag leads to an increase in the number of network units, hence the polymerization will strength in the network structure of the slag (Si–O bonds), increasing the viscosity. (FENG et al., 2019)

It can be concluded that the viscosity increases with the addition of Al_2O_3 when its content is between 15 and 25wt.%. Increasing more the Al_2O_3 content, leads to the replacement of Si-O bond by Al-O bond this lead to a weakening of resistance to the viscous flow, and thus of the viscosity. As presented in the literature, Al_2O_3 presents an amphoteric behavior (ZHANG; CHOU, 2013; KIM et al., 2013; MIN; MEI; XI-DONG, 2011).

As it can be seen in Figures 4.3, 4.4 and 4.5 the viscosity of the slag melt decreases with increasing MgO content from 0 to 15wt.%. This implies that MgO behaves as a network modifier. At C/S wt.ratios of 0.8 and 1.0, the basic components (CaO and MgO) in the slag out-weight the acidic component (SiO_2) when increasing the MgO content. Therefore, the effect of MgO content on the slag viscosity is not much pronounced in this compositions rage.

By comparing the above effects for the different oxides at different tem-

peratures (Figures 4.3, 4.4 and 4.5) we can conclude that, the polymerization and depolymerization of slag structures can also occur at higher temperatures, where the excess thermal energy can provide sufficient energy to break the existing complex network structures, thereby decreasing the viscosity. Thus, at high temperature (arrange 1700°C), the increase of the C/S wt.ratios does not have a significant effect on the depolymerization, as many of the existing complex network structures have already been broken due to the higher thermal energy at 1700ºC compared to 1500ºC, as shown in Figures 4.3, 4.5. Therefore, the polymerization of the slag is strongly affected by the increase in temperature (GAO et al., 2014; ZHANG; CHOU, 2013; KIM et al., 2013; KIM et al., 2010)

4.2.1.2 Liquid/Solid Fraction effect

In order to evaluate the liquid/solid fraction in slag systems with the effect of different chemical composition, 3 graphs were generated, at a temperature of 1500, 1600 and 1700 ºC respectively (Figures 4.6, 4.7 and 4.8). There figures show a gray scale, in which the whiter colored slags are slags with higher liquid fraction and on the other hand the darker slags are slags with higher solid fraction.

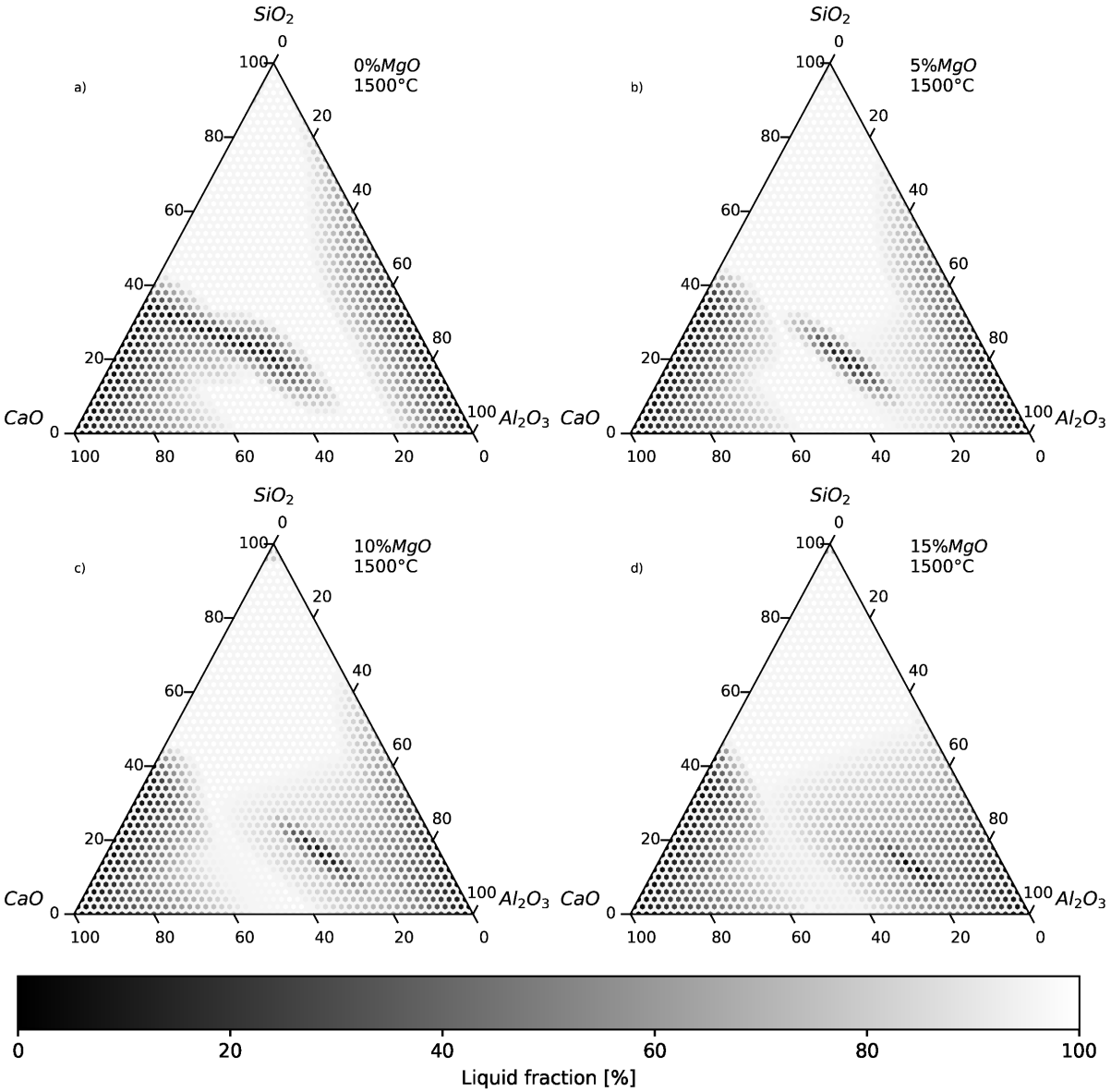

FIGURE 4.6. Liquid/Solid Fraction behavior: (a) CaO-SiO_2-Al_2O_3 system (wt.%); (b) normalized CaO-SiO_2-Al_2O_3–(5%MgO) system (wt.%); (c) normalized CaO-SiO_2-Al_2O_3–(10%MgO) system (wt.%); and (d) normalized CaO-SiO_2-Al_2O_3–(15%MgO) (wt.%), at 1500°C.

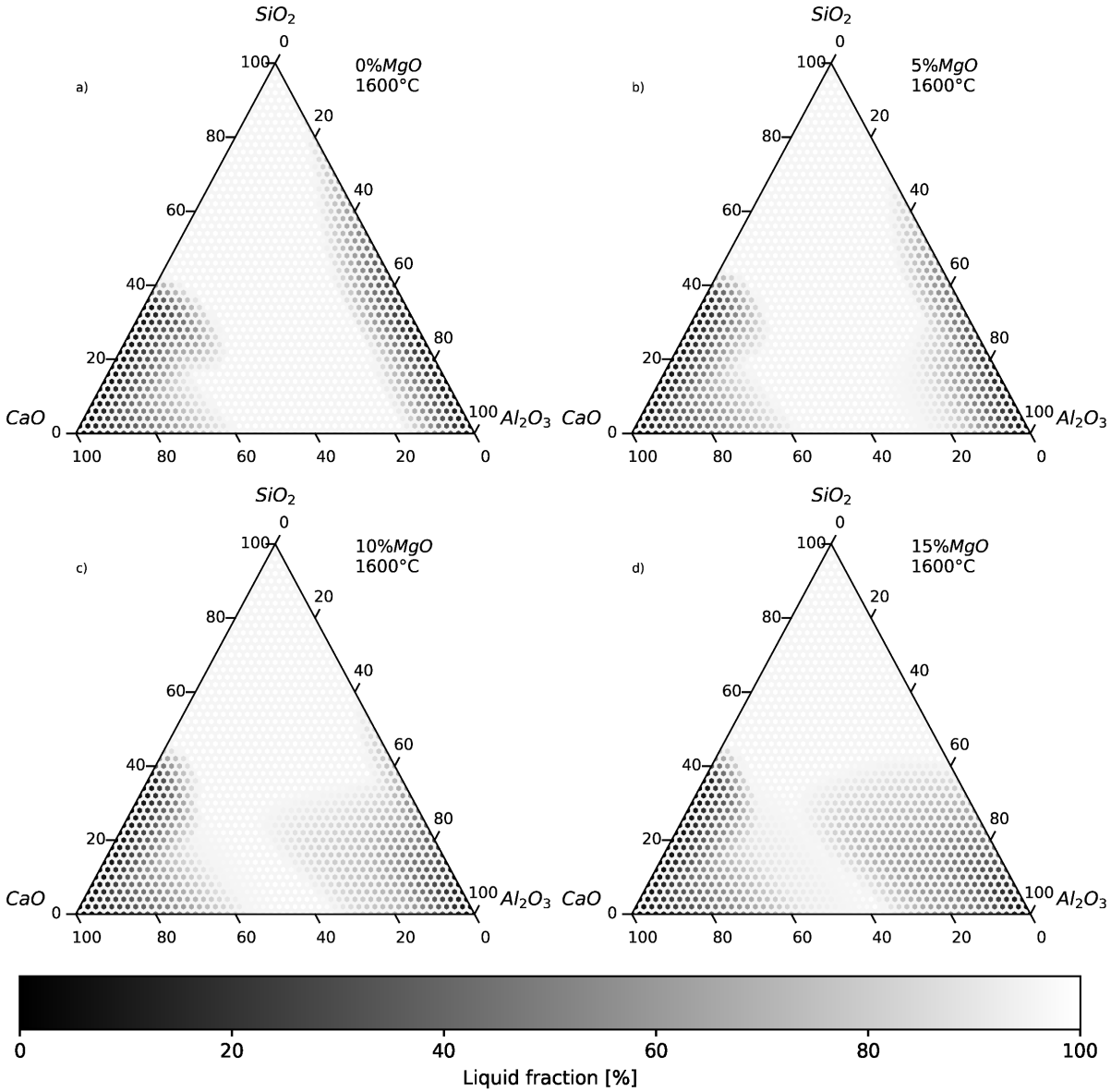

FIGURE 4.7. Liquid/Solid Fraction behavior: (a) CaO-SiO_2-Al_2O_3 system (wt.%); (b) normalized CaO-SiO_2-Al_2O_3–(5%MgO) system (wt.%); (c) normalized CaO-SiO_2-Al_2O_3–(10%MgO) system (wt.%); and (d) normalized CaO - SiO_2 - Al_2O_3–(15%MgO) (wt.%), at 1600°C.

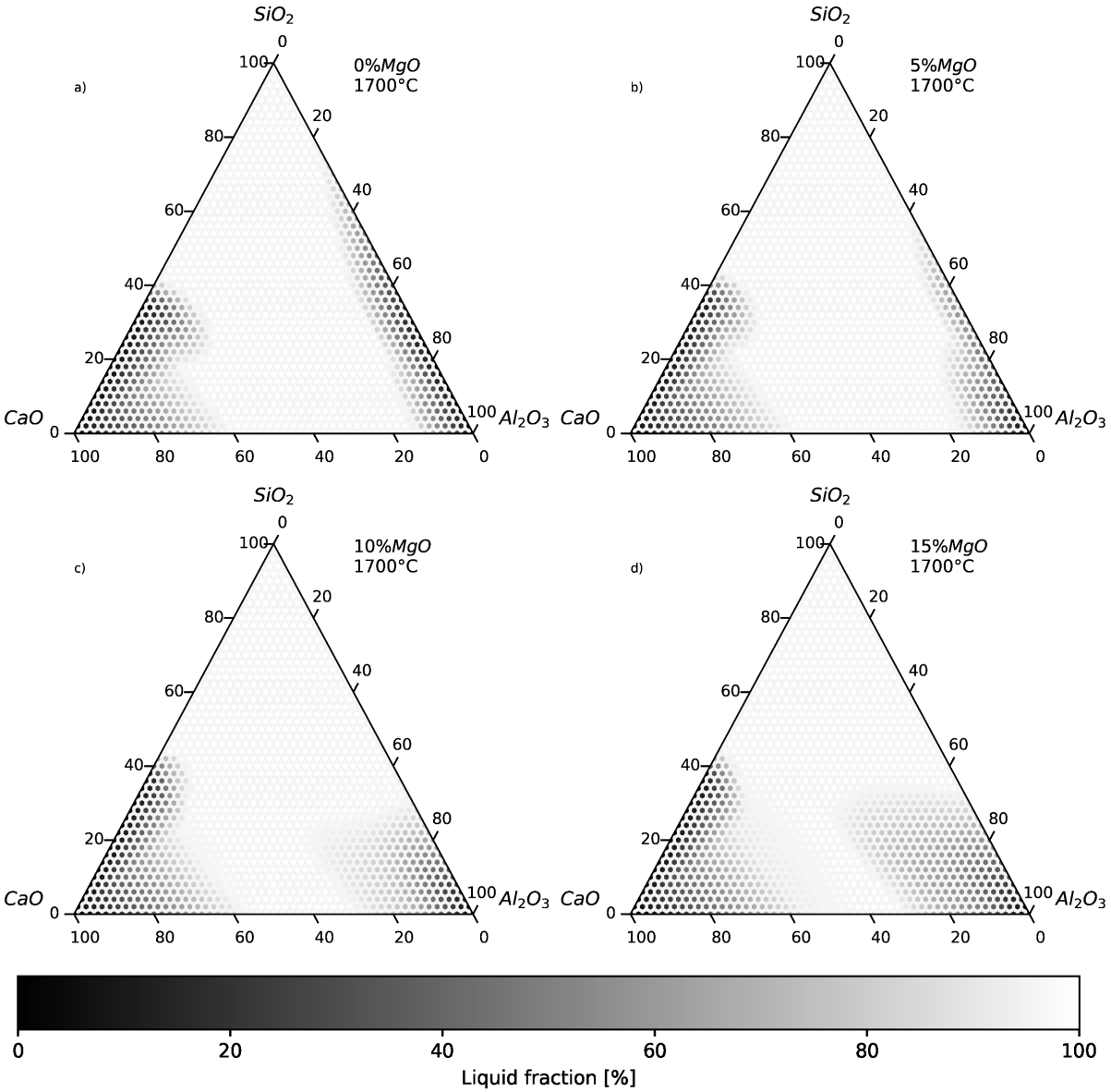

FIGURE 4.8. Liquid/Solid Fraction behavior: (a) CaO-SiO_2-Al_2O_3 system (wt.%); (b) normalized CaO-SiO_2-Al_2O_3–(5%MgO) system (wt.%); (c) normalized CaO-SiO_2-Al_2O_3–(10%MgO) system (wt.%); and (d) normalized CaO - SiO_2 - Al_2O_3–(15%MgO) (wt.%), at 1700°C.

Analyzing the figures above (i.e. Figures 4.6, 4.7 and 4.8), it is possible to conclude the following points:

The addition of CaO significantly increase the liquidus of slag. Due to the high melting point, slags with high content of CaO need high temperatures to be in the liquid state. It can be seen that between a composition range of 20 - 50wt.% CaO the slags are in a liquid state and as the slag temperature increases this slag range increases to 20 - 60wt.% CaO. At high contents of MgO (10 - 15wt.%), the depolymerization is intensified and this range of CaO compositions in liquid phase is increased. Slags with C/S wt.ratios less than 1 will be in the liquid state. However, at C/S wt.ratios of 0.8 and 1.0, as the basic components (CaO and MgO) in the slag outweigh the acidic component (SiO_2) with increasing MgO content, many of the network structures have already been depolymerized. Therefore, the effect of the MgO content on the liquid slag fraction is impaired.

The effect of adding SiO_2 is an increase in the liquid fraction of basic slag system, because SiO_2 has a low melting point. With the increase of MgO it is possible to see an increase in the liquid part because the magnesium oxide acts as a network modifier.

The addition of Al_2O_3 also increases the liquidus of many slag system. This occurs due to the high melting point of alumina. It is possible to notice that the increase of the solid fraction with alumina higher than 40wt.%, and this effect is intensified when the system has MgO content greater than 5wt.% in the composition.

The Liquid Phase is gradually reduced, with increases in the MgO content, as seen in past work (KIM et al., 2010; GAO et al., 2014; GAN; XIN; ZHOU, 2017).

By comparing the above effects for the different oxides at different temperatures it can conclude that, Figures 4.6, 4.7, 4.8, the increase in temperature, increases the liquid zone of the slag.

4.2.2 Temperature influence

The effect of rising the temperature on the viscosity of slags will be discussed in this chapter. The impact it has an liquid/solid fraction will also be presented.

4.2.2.1 Viscosity effect

To evaluate the effect of the temperature on the slag viscosity of slag, 3 graphs were made, by subtracting the slag viscosity at 2 different temperatures with the same chemical composition at thus temperatures. The first graph shows the viscosity difference, in [Pa.S], of the same slags between 1600 and 1500°C, Figure 4.9. The second graph show the viscosity difference, in [Pa.S], between 1700 and 1600°C, Figure 4.10; and finally show the difference, in [Pa.S], between 1700-1500°C , Figure 4.11. The figures show a rainbow color scale of negative values, because it is expected that with increasing temperature the viscosities will decrease, so subtraction will result in negative values.

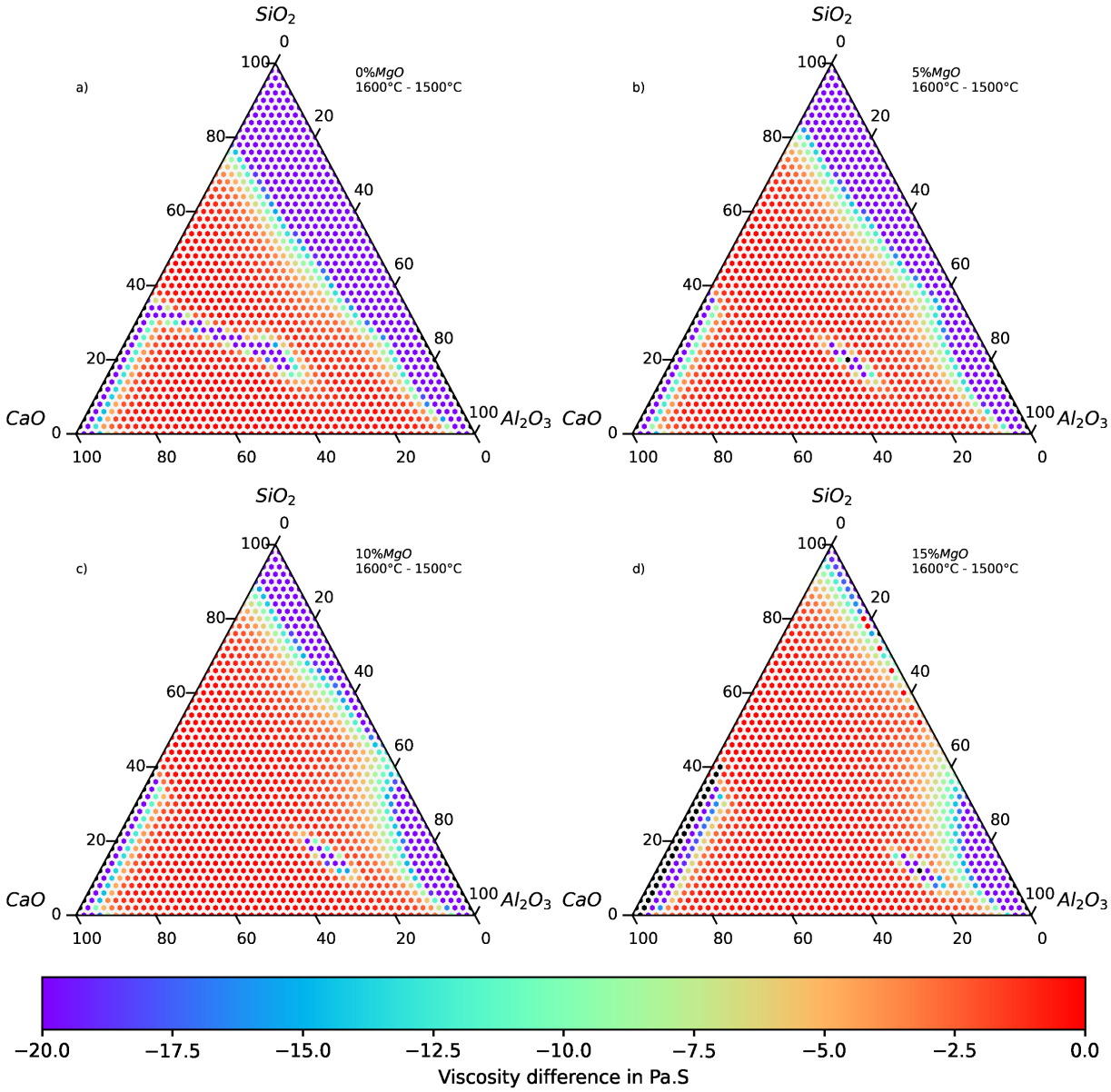

FIGURE 4.9. Viscosity difference in [Pa.S]: (a) CaO-SiO_2-Al_2O_3 system (wt.%); (b) normalized CaO-SiO_2-Al_2O_3–(5%MgO) system (wt.%); (c) normalized CaO-SiO_2-Al_2O_3–(10%MgO) system (wt.%); and (d) normalized CaO - SiO_2 - Al_2O_3–(15%MgO) (wt.%), between 1600 - 1500°C.

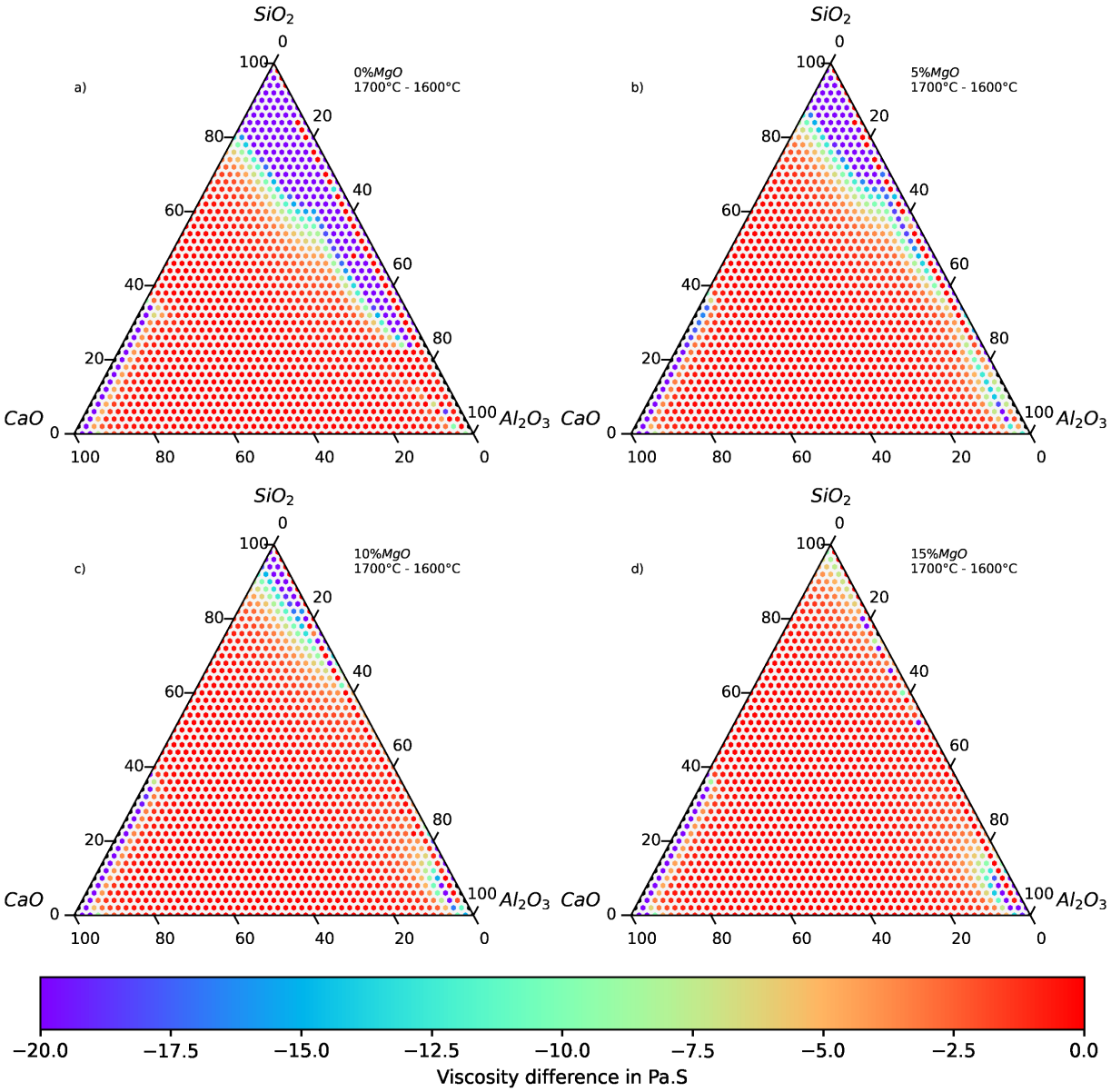

FIGURE 4.10. Viscosity difference in [Pa.S]: (a) CaO-SiO_2-Al_2O_3 system (wt.%); (b) normalized CaO-SiO_2-Al_2O_3–(5%MgO) system (wt.%); (c) normalized CaO-SiO_2-Al_2O_3–(10%MgO) system (wt.%); and (d) normalized CaO - SiO_2 - Al_2O_3–(15%MgO) (wt.%), between 1700 - 1600°C.

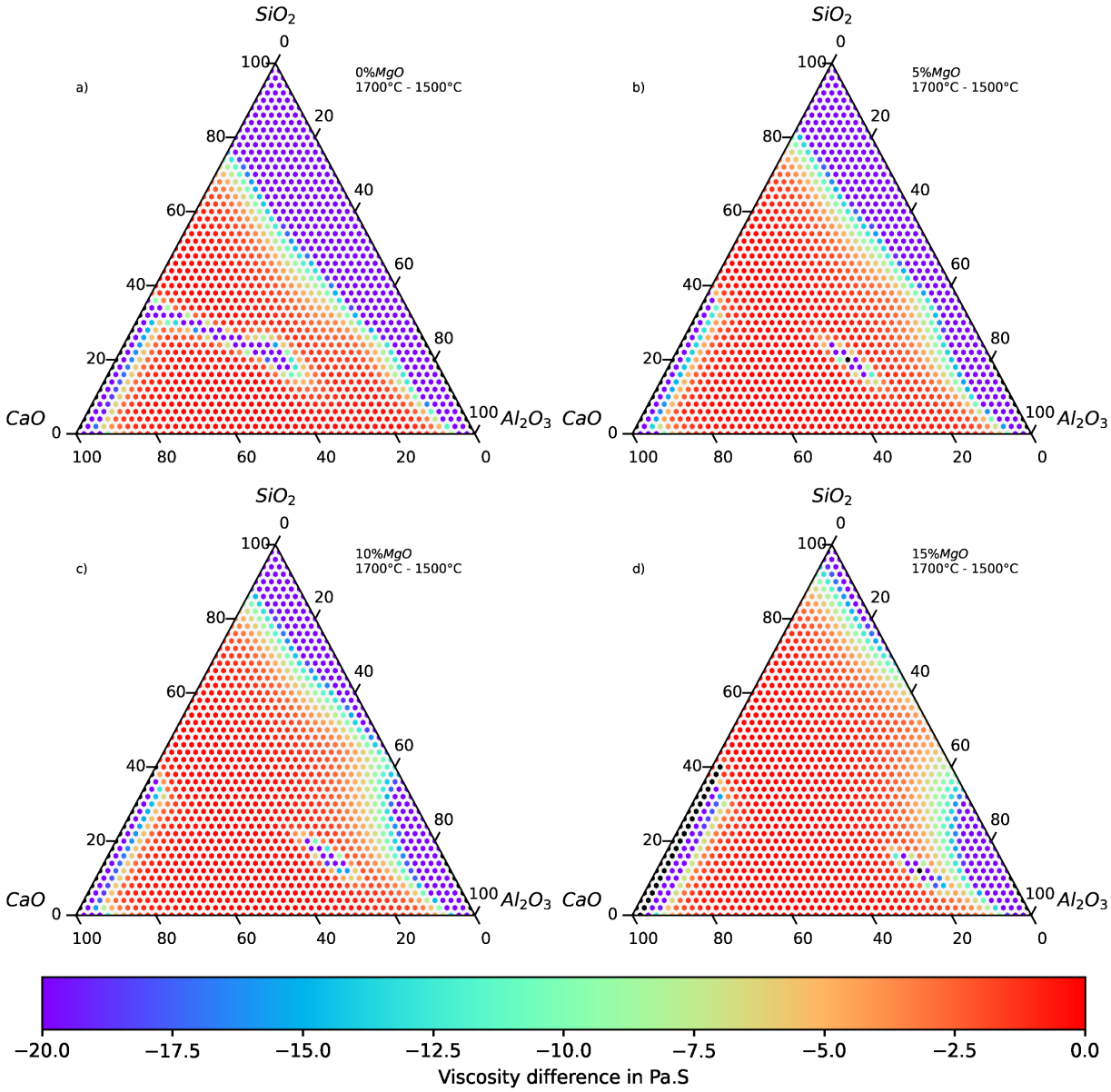

FIGURE 4.11. Viscosity difference in [Pa.S]: (a) CaO-SiO_2-Al_2O_3 system (wt.%); (b) normalized CaO-SiO_2-Al_2O_3–(5%MgO) system (wt.%); (c) normalized CaO-SiO_2-Al_2O_3–(10%MgO) system (wt.%); and (d) normalized CaO - SiO_2 - Al_2O_3–(15%MgO) (wt.%), between 1700 - 1500°C.

In Figure 4.9, it can be seen that the effect of increasing the temperature

by 100 degrees, starting at 1500°C, resulted in the reduction of the viscosity of slags. For low basicity slags, the effect was not as clear for C/S wt.ratios greater than 1. The effect of the addition of MgO ends up not intensifying the effect of the reduction of the viscosity of the slag in the increase of the temperature, because as the magnesium oxide acts as a depolymerizer in the slag, then with the presence of MgO the slag presents a breaking point at lower temperatures, then its viscosity already presents its lower plateau for lower temperatures. Therefore, the temperature effect is not so relevant (GAO et al., 2014).

Figure 4.10 shows the effect of increasing the slag by 100 degrees starting at 1600 degrees. It was possible only to visualize the decrease in viscosity for the slags with C/S wt.ratios less than 1. With the increase of MgO there were no significant decrease in viscosity caused by the temperature increase, because MgO performs as a network "modifier" and the oxide leads the viscosity to reach the breaking point (KIM et al., 2010).

Performing an overview of the increase of temperature from 1500 to 1700 degrees, Figure 4.11 ,it is possible to visualize that the viscosity was in general reduced when increasing temperature.

4.2.2.2 Liquid/Solid Fraction

To evaluate the increase of the liquid fraction in the slag with increasing temperature, this chapter will consist of a subtraction in the liquid fraction of the slag for the same chemical compositions with different temperatures. The first graph will be the subtraction, of the liquid fraction in [%], of the same slag between the temperature of 1600 and 1500°C, Figure 4.12 ,the second graph will be the subtraction between the temperatures 1700 and 1600°C, Figure 4.13 and finally the subtraction between the temperatures 1700-1500°C, Figure 4.14. The figures show a color scale between blue and red, in which slags that show

a more red coloration are slags that showed a gain in the liquid fraction, and slags in blue are slags that did not get a gain in the liquid fraction.

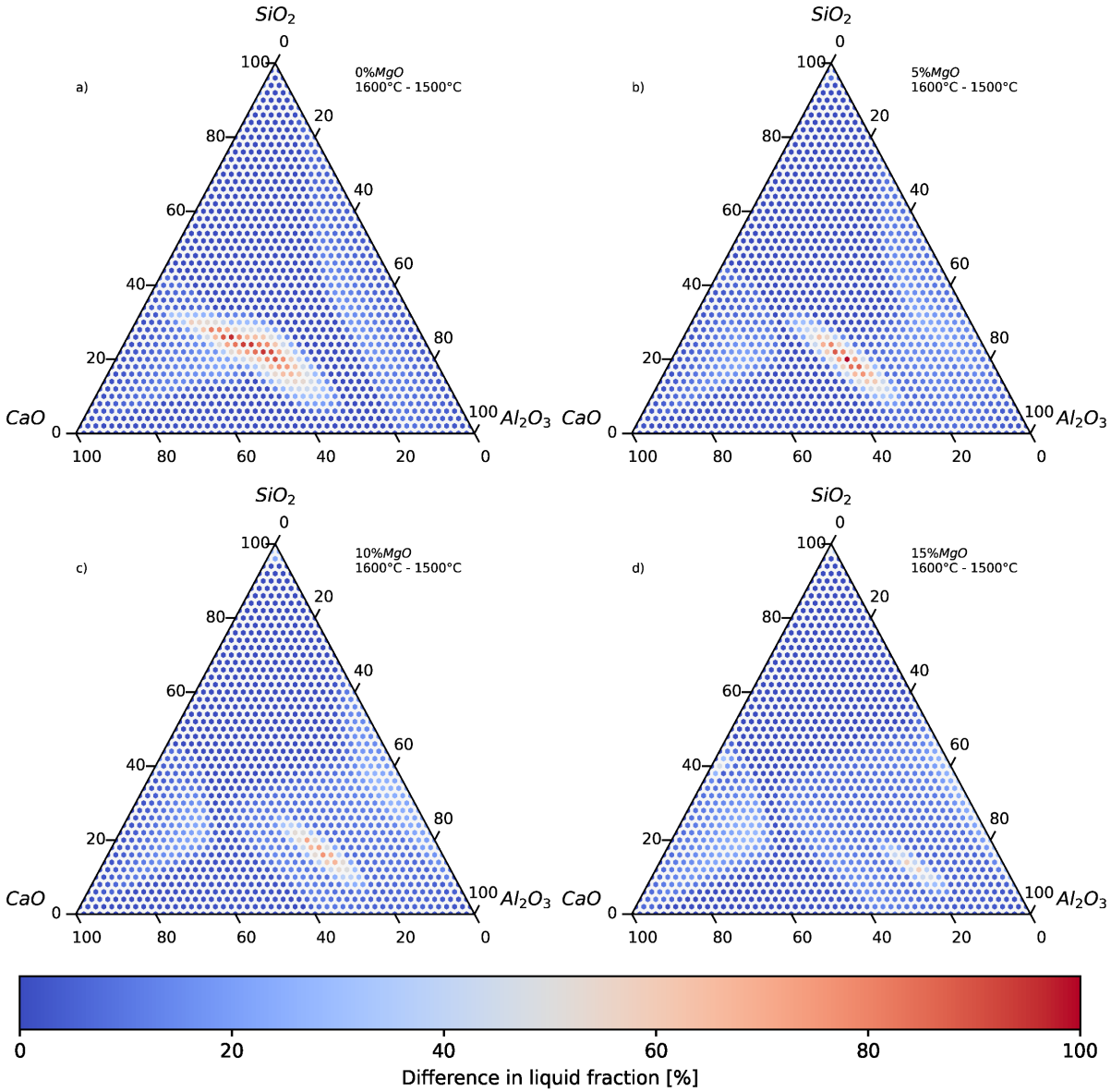

FIGURE 4.12. Liquid Fraction difference: (a) CaO-SiO_2-Al_2O_3 system (wt.%); (b) normalized CaO-SiO_2-Al_2O_3–(5%MgO) system (wt.%); (c) normalized CaO-SiO_2-Al_2O_3–(10%MgO) system (wt.%); and (d) normalized CaO - SiO_2 - Al_2O_3–(15%MgO) (wt.%), between 1600 - 1500°C.

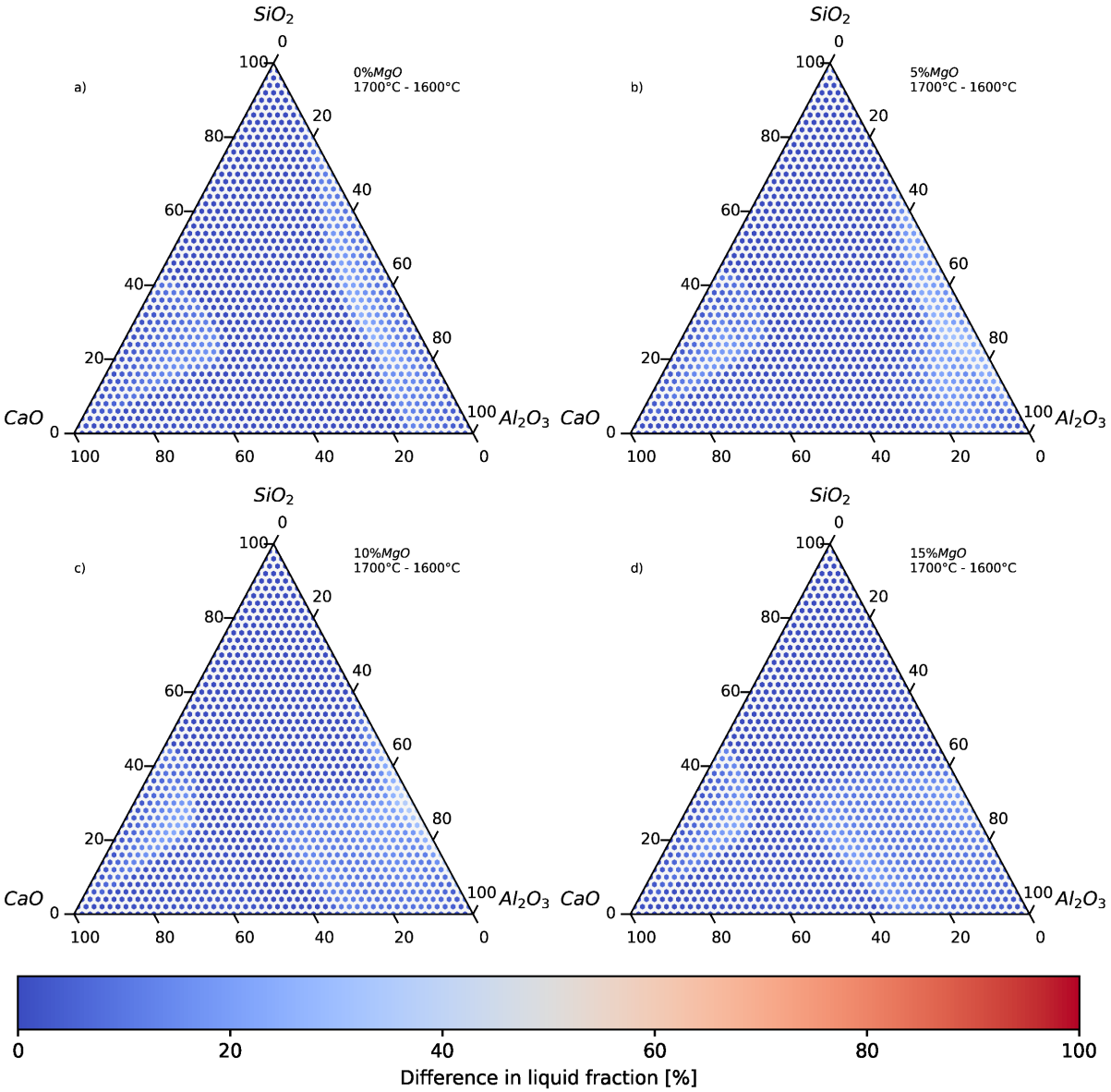

FIGURE 4.13. Liquid Fraction difference: (a) CaO-SiO_2-Al_2O_3 system (wt.%); (b) normalized CaO-SiO_2-Al_2O_3–(5%MgO) system (wt.%); (c) normalized CaO-SiO_2-Al_2O_3–(10%MgO) system (wt.%); and (d) normalized CaO - SiO_2 - Al_2O_3–(15%MgO) (wt.%), between 1700 - 1600°C.

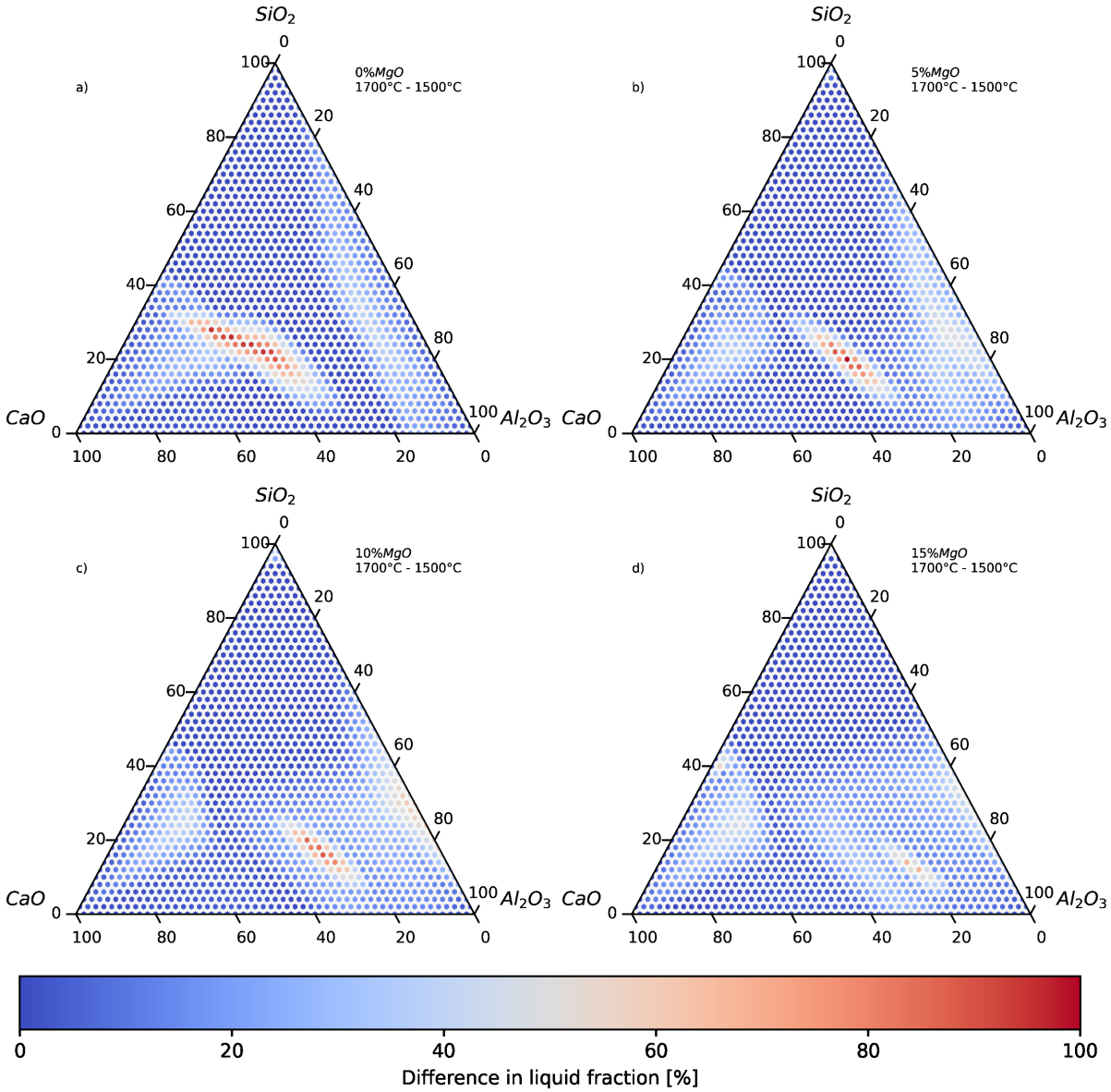

FIGURE 4.14. Liquid Fraction difference: (a) CaO-SiO_2-Al_2O_3 system (wt.%); (b) normalized CaO-SiO_2-Al_2O_3–(5%MgO) system (wt.%); (c) normalized CaO-SiO_2-Al_2O_3–(10%MgO) system (wt.%); and (d) normalized CaO - SiO_2 - Al_2O_3–(15%MgO) (wt.%), between 1700 - 1500°C.

This section presents the visualizing of the effect of increasing by 100 degrees the temperature of slag on the increase of the liquid fraction of the slag. It

is possible to visualize that the slags that were at 1500 temperature and heated to 1600º presented an increase on their liquid fraction for silica-alumina slags, and for slags with high concentration of CaO (see red the elliptical shape resign that will be discussed in the next chapters). Another observation is that slags with 5% MgO did not show an increase of its liquid fraction because oxide presents itself as a network modifier and were finally liquid at low temperature. At important MgO addition (10-15wt.% MgO) the slag will present an excess of network modifiers and the temperature increase will be necessary to reach the liquidus of the system.

In Figure 4.13 it is possible to see the effect of raising the slag temperature from 1600ºC to 1700ºC. It is possible to conclude that the increase in the liquid fraction is only notable for high alumina or high CaO zones, because these systems have high liquidus temperature.

The overall effect of increasing the temperature by 200ºC is seen in Figure 4.14. It is possible to see zones that presented a substantial increase in the liquid fraction with temperature.

4.2.3 Iso-viscosity curves

The iso-viscosity curves for the CSAM system are presented at different content of MgO and for 3 different temperatures (1500°C,1600°C,1700°C), in Figures 4.15,4.16,4.17. The figures show a gray scale representing the liquid fraction, a line in gold coloration representing the liquidus line of the slag, and the viscosity iso-curves in dashed lines in blue color.

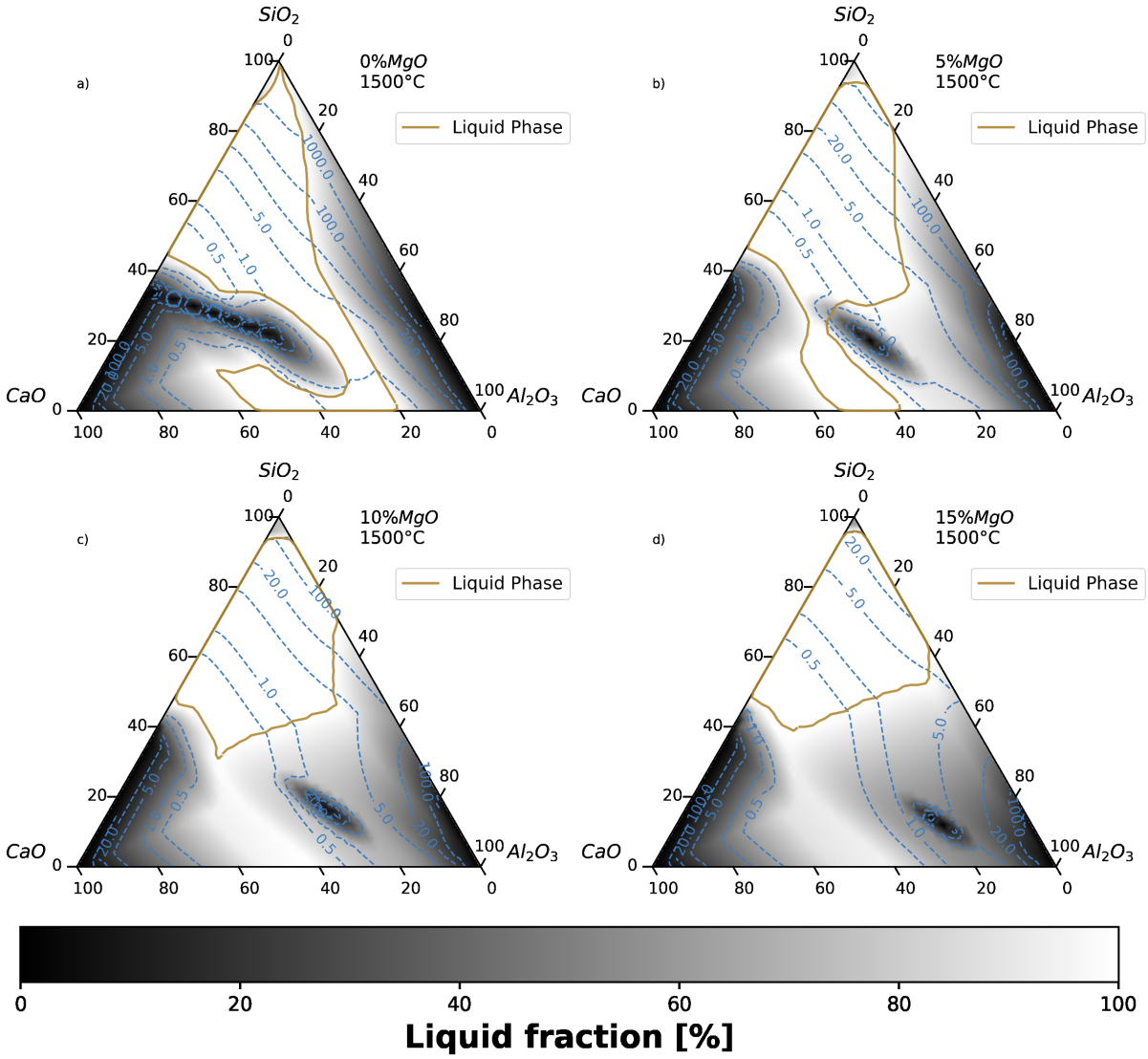

FIGURE 4.15. Iso-viscosity [Pa.s] curves of slags in Liquid and Two-Phase regions: (a) CaO-SiO_2-Al_2O_3 system (wt.%); (b) normalized CaO-SiO_2-Al_2O_3–(5%MgO) system (wt.%); (c) normalized CaO-SiO_2-Al_2O_3–(10%MgO) system (wt.%); and (d) normalized CaO - SiO_2 - Al_2O_3–(15%MgO) (wt.%), at 1500°C.

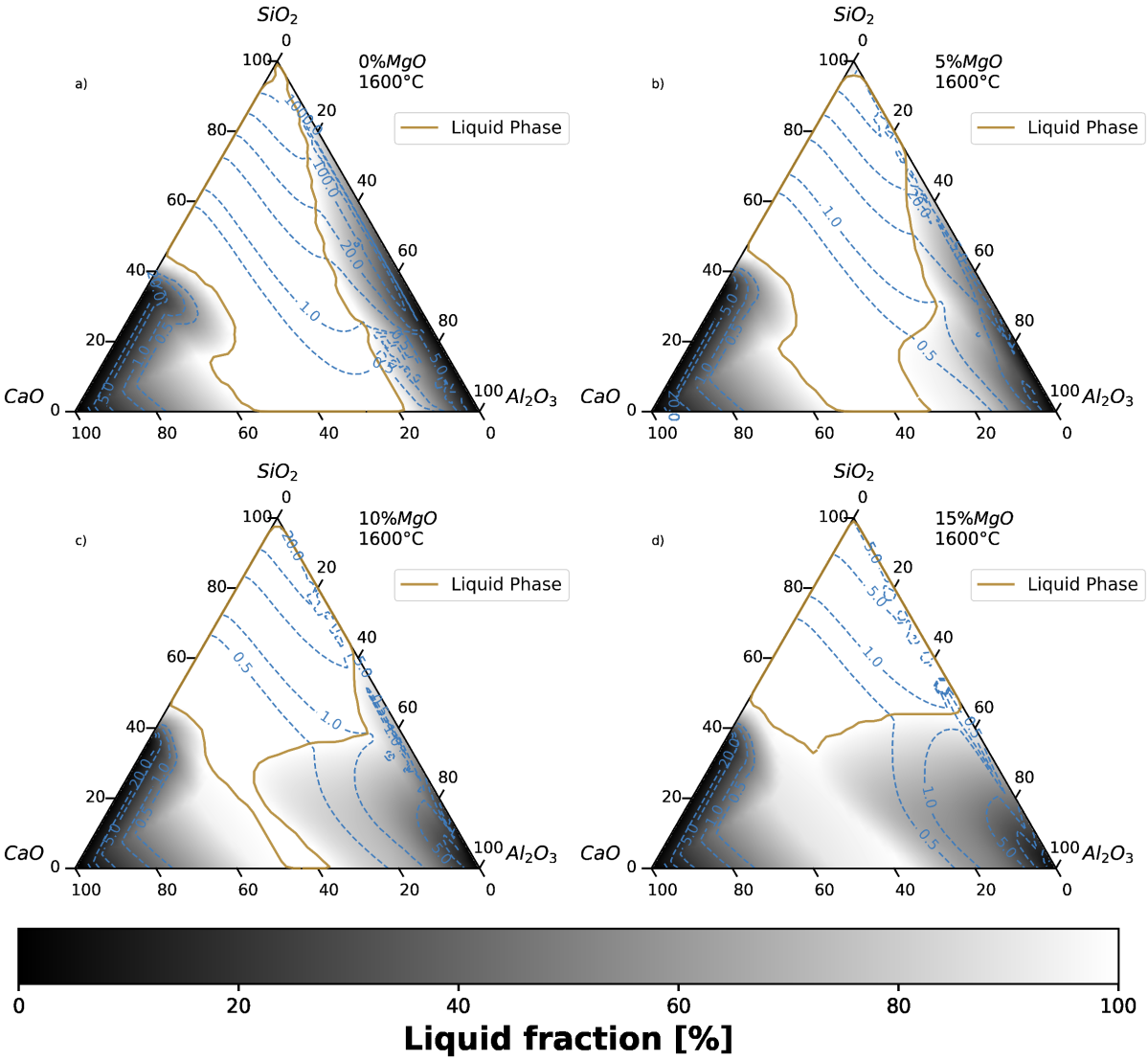

FIGURE 4.16. Iso-viscosity [Pa.s] curves of slags in Liquid and Two-Phase regions: (a) CaO-SiO_2-Al_2O_3 system (wt.%); (b) normalized CaO-SiO_2-Al_2O_3–(5%MgO) system (wt.%); (c) normalized CaO-SiO_2-Al_2O_3–(10%MgO) system (wt.%); and (d) normalized CaO - SiO_2 - Al_2O_3–(15%MgO) (wt.%), at 1600°C.

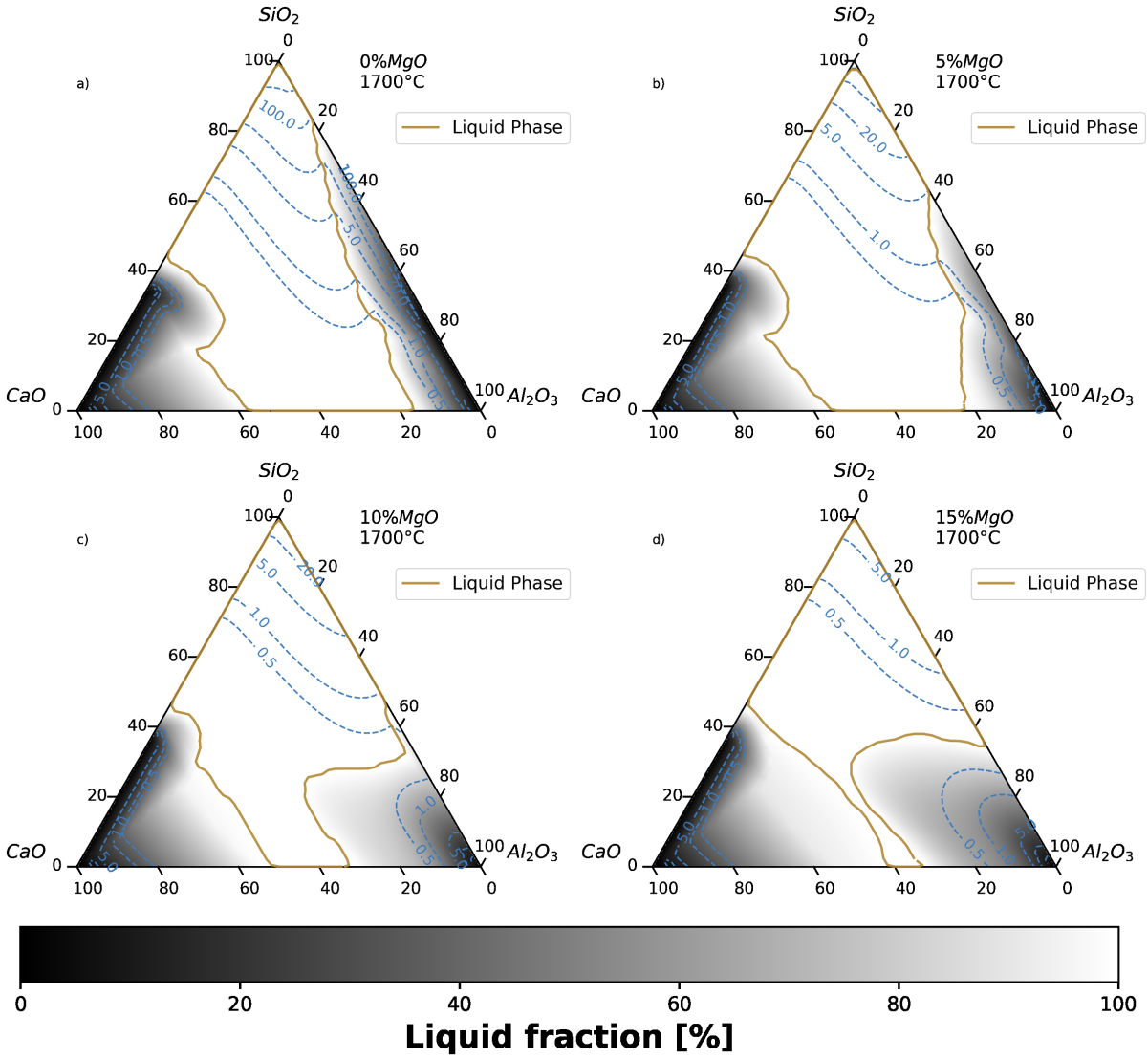

FIGURE 4.17. Iso-viscosity [Pa.s] curves of slags in Liquid and Two-Phase regions: (a) CaO-SiO_2-Al_2O_3 system (wt.%); (b) normalized CaO-SiO_2-Al_2O_3–(5%MgO) system (wt.%); (c) normalized CaO-SiO_2-Al_2O_3–(10%MgO) system (wt.%); and (d) normalized CaO - SiO_2 - Al_2O_3–(15%MgO) (wt.%), at 1700°C.

The analysis of these figures (Figures 4.15, 4.16 and 4.17), show that an increase of MgO content decrease the viscosity. MgO is a network "modifier",

and thus decreases the viscosity of these lags at a given temperature (GAO et al., 2014). The Liquid fraction is gradually reduced, with an increase in the MgO content, as confirmed by the experimental data in the literature (GAN; XIN; ZHOU, 2017). Additionally, it is also revealed in Figure 4.15, 4.16 and 4.17 that the low viscosity area (0 - 1Pa.s) are much larger in slags with high MgO contents and for higher temperatures.

Figure 4.15 show that an it can be seen that with increase in the solid fraction leads to a drastic increase in viscosity, as predicted by Equation 3.1.

With the increase of the solid fraction, there is a distortion in the iso-viscosity curves, because of the resulting increase in the slag viscosity.

It is possible to visualize an influence of a solid solution in the slag at 1500ºC , Figure 4.15, increasing the viscosity of the slag. This effect will be discussed in the next chapter 4.2.3.1.

4.2.3.1 Melilite influence

The phase assemblage in Figure 4.15 a) in the area of 40 - 70% CaO, 20 - 40% SiO_2, and 0 - 40% Al_2O_3, consists of a large fraction of solid which increased viscosity.

In order to explain this effect, Figure 4.18 shows phase equilibria at 1500ºC for these different slag compositions.

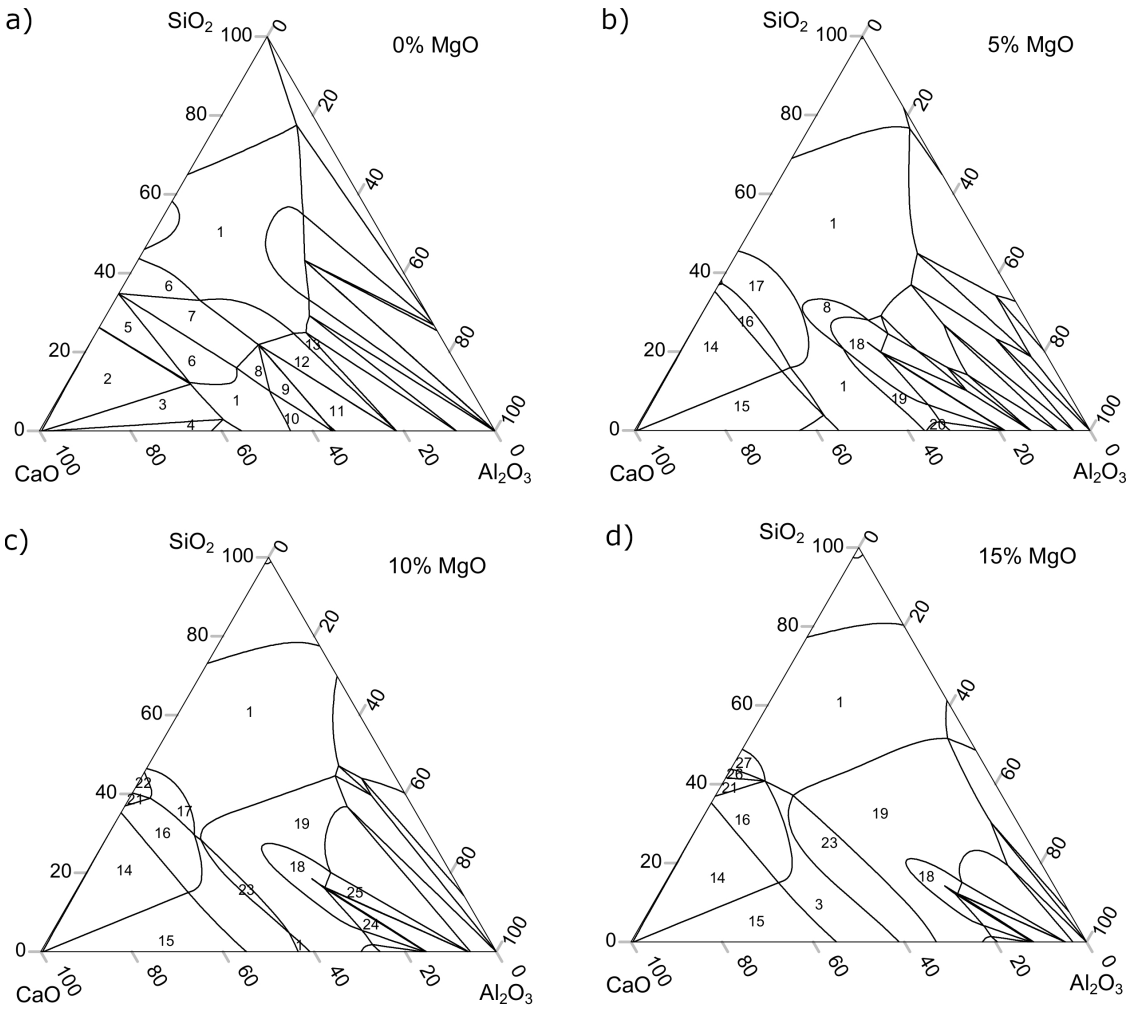

1	Slag−liq	10	CaAl{2}O{4} + Slag−liq	19	Slag−liq + Spinel
2	Ca{3}SiO{5} + Monoxide + Slag−liq	11	CaAl{2}O{4} + CaAl{4}O{7} + Melilite	20	CaAl{2}O{4}+ Slag−liq + Spinel
3	Monoxide + Slag−liq	12	CaAl{4}O{7} + Melilite + Slag−liq	21	Ca{3}MgSi{2}O{8} + Monoxide + Slag−liq + a−(Ca,Sr)2SiO4
4	Ca{3}Al{2}O{6} + Monoxide + Slag−liq	13	CaAl{4}O{7} + Slag−liq	22	Ca{3}MgSi{2}O{8} + Slag−liq + a−(Ca,Sr)2SiO4
5	Ca{2}SiO{4}(s3) + Ca{3}SiO{5} + Slag−liq	14	Monoxide + Monoxide#2 + Slag−liq + a−(Ca,Sr)2SiO4	23	Monoxide + Slag−liq + Spinel
6	Ca{2}SiO{4}(s3) + Slag−liq	15	Monoxide + Monoxide#2 + Slag−liq	24	CaAl{4}O{7} + Melilite + Slag−liq + Spinel
7	Ca{2}SiO{4}(s3) + Melilite + Slag−liq	16	Monoxide + Slag−liq + a−(Ca,Sr)2SiO4	25	CaMg{2}Al{1}{6}O{2}{7} + Melilite + Slag−liq + Spinel
8	Melilite + Slag−liq	17	Slag−liq + a−(Ca,Sr)2SiO4	26	Ca{3}MgSi{2}O{8} + Monoxide + Slag−liq
9	CaAl{2}O{4} + Melilite + Slag−liq	18	Melilite + Slag−liq + Spinel	27	Ca{3}MgSi{2}O{8} + Slag−liq

FIGURE 4.18. Equilibrium phases presents in the Liquid and Two-Phase regions: (a) CaO-SiO_2-Al_2O_3 system (wt.%); (b) normalized CaO-SiO_2-Al_2O_3–(5%MgO) system (wt.%); (c) normalized CaO-SiO_2-Al_2O_3–(10%MgO) system (wt.%); and (d) normalized CaO - SiO_2 - Al_2O_3–(15%MgO) (wt.%), at 1500°C.

The (slag-liq) represents the region of single-phase slag, while all the other zones present same solid phases. According to the Figure 4.18, Melilite ((Ca_2(Al,Mg,Fe^{2+}), $(Si, Al)_2\ O_7$) is present in many regions (7, 8, 9, 11, 12, 18, 24, 25) and increases the viscosity of the slag system, as seen in Figure 4.15. Melilite in CAIs consists almost exclusively of the binary solid solution gehlenite [$Ca_2Al_2SiO_7$]–akermanite [$Ca_2MgSi_2O_7$]. The melting point of gehlenite is 1593°C and 1454°C for akermanite. (MACPHERSON, 2007)

Correlating Figure 4.15 with Figure 4.18 is possible to see that the increase of the solid fraction is connected to the presence of the Melilite phase. The increases of MgO stabilizes the Melilite phase to lower CaO, SiO_2, and higher Al_2O_3 contents. With increasing MgO concentration, the melilite phase will contain mostly the akermanite, which has a lower melting point, thus slags with higher MgO concentration will limit the solid fraction effect induced by the melilite phase formation.

Visualizing Figure 4.12 it is possible to see that with the increase of 100 degrees there is an increase in the liquid fraction in the zones where the melilite is found. Correlated with Figure 4.7, it is possible to notice that the solid phase became a liquid phase.

4.2.3.2 Thermal and Chemical Influence

This last section discusses the effect of the chemical composition and temperature on the low viscosity zones (0-1 Pa.s) and liquid zones of the slag. Figure 4.19 was specifically built for this discussion, in this figure we compare 3 different temperatures (1500, 1600 and 1700°C) in relation to the low viscosity zones and the liquid zone of the slag. Each temperature has two with similar colors, where the liquid zone is represented by a solid line and the low viscosity zone is represented by a dashed line.

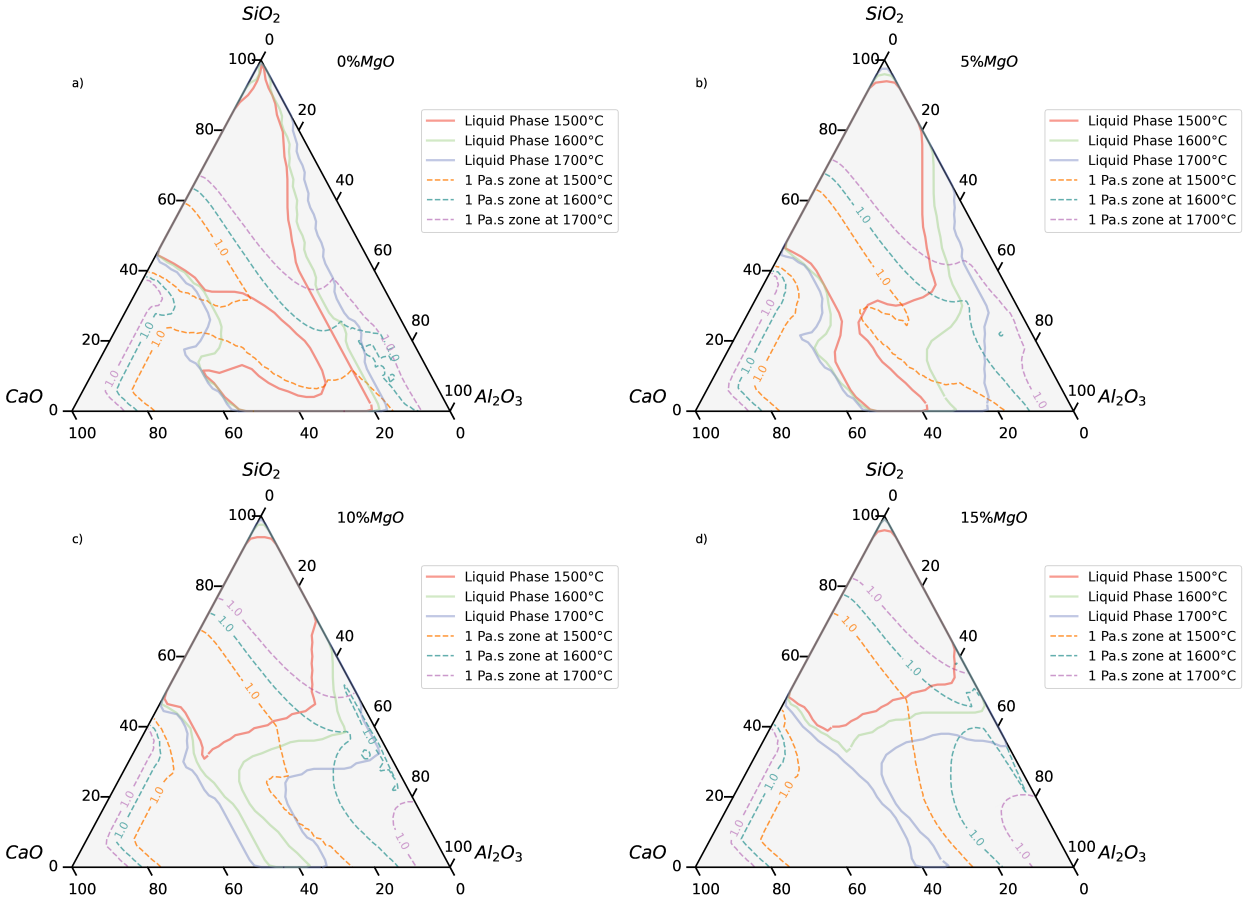

FIGURE 4.19. Thermal and chemical Influence on low viscosity zones(0-1 Pa.s) for temperatures 1500, 1600 and 1700ºC: (a) CaO-SiO_2-Al_2O_3 system (wt.%); (b) normalized CaO-SiO_2-Al_2O_3–(5%MgO) system (wt.%); (c) normalized CaO-SiO_2-Al_2O_3–(10%MgO) system (wt.%); and (d) normalized CaO - SiO_2 - Al_2O_3–(15%MgO) (wt.%).

Analyzing Figure 4.19 it is possible to see that the increase in temperature generates an increase in the size of low viscosity zones associated to an increase in the liquid zone of the slag. This confirms all previous observations. The increase in MgO reduces the viscosity of the slag and also increases the size of the low viscosity zone. On the other hand, the addition of the MgO results in a decrease in the liquid zone.

Chapter 5

Conclusions

In summary, FactSage 7.3 was employed to analyze the behavior of slags for the CSAM systems at 1500ºC, 1600°C and 1700°C the Rocoe-Einstin was used to predict the viscosity of slags containing solid fractions. The calculated data were compared with the experimental data collected in many references cited in this work. About 570 experimental data were collected to compare the data with the calculated values, we propose an accurate representation of iso-viscosity curves applied for secondary steelmaking slags. The following main conclusions can be drawn from this work:

- A comparison between the viscosity data collected from the literature with the viscosities calculated by FactSage shows a mean percent error lower than the 30% mean percent error typically obtained during viscosity measurement.
- By the analysis proposed, it is possible to visualize that the effect of the MgO content (0-15%wt.) decreases the viscosity. As a further observation, increasing MgO showed an increase in the size of the low viscosity zones (0-1Pa.s).
- The effect of the CaO oxide showed a significant viscosity decreases for C/S wt.ratios less than 1, but higher amounts of CaO had a limited im-

panct an melt viscosities. CaO additions between 20% and 60%wt. lead to an increase in the liquid fraction of the slag. At higher content of CaO (>60%wt.) there is an increase in the solid fraction.

- Al_2O_3 showed amphoteric behavior, increasing viscosity at 15-25%wt. and decreasing viscosity at high concentrations. Although it is possible to notice the increase of the solid fraction with alumina higher than 40%wt., this effect intensified when the system has MgO content greater than 5%wt.

- The FactSage 7.3 sotware was great help in the creation of pseudo ternary systems with iso-viscosity curves. This is a useful representation for steelmakers, considering the slag designing process, aiming at obtaining the best conditions of steel refining.

Chapter 6

Recommendations for Future Work

There are limited iso-curves of viscosity available in the literature for slags at high temperature. For this reason, the present work will be continued in order to gather new results. Many new areas can yet be explored, and some points from this work further clarified. Some ideas along these lines are presented below.

1. Use the methodology of the present work and include Fluorite, CaF_2, in the slag systems.

2. Develop a comparative study with experimental viscosity measurements with the graphs generated from the iso-viscosity curves.

3. Apply the knowledge acquired in the construction of iso-viscosity curve diagrams for the ability to remove inclusions for different slag compositions.

4. Visualize the effects of each oxide on viscosity by two-dimensional plots for several temperatures.

5. Use the methodology of this present work and include Iron(II) oxide, FeO, in the slag systems.

6. Employ the built algorithm for calculating iso-viscosity curves for other areas of Materials knowledge, such as polymers.

References

ASTH, H. G. *UNIVERSIDADE FEDERAL DE MINAS GERAIS DESENVOLVIMENTO DE ESCÓRIAS DE REFINO SECUNDÁRIO PARA O FORNO PANELA DA VM DO BRASIL*. 2011. Disponível em: <http://hdl.handle.net/1843/BUOS-8TRLRG>.

BALE, C. W. et al. Reprint of: Factsage thermochemical software and databases, 2010–2016. *Calphad: Computer Coupling of Phase Diagrams and Thermochemistry*, Elsevier, v. 55, p. 1–19, 2016. ISSN 03645916. Disponível em: <http://dx.doi.org/10.1016/j.calphad.2016.05.002>.

BIELEFELDT, W. V. et al. *THERMODYNAMIC EVALUATION OF THE SLAG SYSTEM CaO-MgO-SiO*. 2014.

BIELEFELDT, W. V.; VILELA, A. C. F. Study of inclusions in high sulfur, al-killed ca-treated steel via experiments and thermodynamic calculations. *Steel Research International*, Wiley-VCH Verlag, v. 86, p. 375–385, 4 2014. ISSN 16113683.

CHEN, G. J.; HE, S. P. Effect of mgo content in slag on dephosphorisation in converter steelmaking. *Ironmaking Steelmaking*, v. 42, p. 433–438, 2015. ISSN 0301-9233. Disponível em: <http://www.tandfonline.com/doi/full/10.1179/1743281214Y.0000000246>.

CHEN, M.; ZHAO, B. Viscosity measurements of the sio 2 – k 2 o – cao system relevant to biomass slags. *Fuel*, v. 180, p. 638–644, 2016.

CHOPRA, S.; TANEJA, C. Utilization of the indian blast furnace slags. In: NATIONAL METALLURGICAL LABORATORY JAMSHEDPUR. *SYMPOSIUM ON UTILIZATION OF METALLURGICAL WASTES*. [S.l.], 1964. p. 224–225.

DIETZEL, A. Die kationenfeldstärken und ihre beziehungen zu entglasungsvorgängen, zur verbindungsbildung und zu den schmelzpunkten von silicaten. 1942.

DIPPENAAR, R. Industrial uses of slag (the use and re-use of iron and steelmaking slags). *Ironmaking and Steelmaking*, v. 32, p. 35–46, 2 2005. ISSN 03019233.

EINSTEIN, A. Eine neue bestimmung der moleküldimensionen. *Annalen der Physik*, v. 324, p. 289–306, 1906. ISSN 00033804. Disponível em: <http://doi.wiley.com/10.1002/andp.19063240204>.

EINSTEIN, A. Berichtigung zu meiner arbeit: "eine neue bestimmung der moleküldimensionen". *Annalen Der Physik*, p. 591–592, 1911.

ERICSSON, O. T.; KARASEV, A. V.; JöNSSON, P. G. Effect of slag protection system and sample geometry on homogeneity of total oxygen content in samples from liquid steel. *Steel Research International*, v. 82, p. 222–229, 3 2011. ISSN 16113683.

FENG, C. et al. Effects of cao/sio 2 on viscous behaviors and structure of cao-sio 2 -11.00wt%mgo-11.00wt%al 2 o 3 -43.00wt%tio 2 slag systems. *ISIJ International*, Iron and Steel Institute of Japan, v. 59, p. 31–38, 1 2019. ISSN 09151559.

FORSBACKA, L. et al. Experimental study and modelling of viscosity of chromium containing slags. *steel research international*, v. 78, n. 9, p. 676–684, 2007. Disponível em: <https://onlinelibrary.wiley.com/doi/abs/10.1002/srin.200706269>.

FRUEHAN, F. J. *UNIQUE FUNCTIONS OF SLAGS IN STEELMAKING*. 2004.

FUHR, F. et al. Application of slag tracers to investigate source of non-metallic inclusions. *Ironmaking & Steelmaking*, Taylor Francis, v. 34, n. 6, p. 463–470, 2007. Disponível em: <https://doi.org/10.1179/174328107X174609>.

GAN, L.; XIN, J.; ZHOU, Y. Accurate viscosity calculation for melts in sio₂–al₂o₃–cao–mgo systems. *ISIJ International*, v. 57, p. 1303–1312, 2017. ISSN 0915-1559.

GAO, Y. M. et al. Effects of basicity and mgo content on the viscosity of the sio2-cao-mgo-9wt*International Journal of Minerals, Metallurgy and Materials*, v. 21, p. 353–362, 2014. ISSN 1869103X.

GHERIBI, A. E. et al. Calculating optimal conditions for alloy and process design using thermodynamic and property databases, the factsage software and the mesh adaptive direct search algorithm. *Calphad: Computer Coupling of Phase Diagrams and Thermochemistry*, v. 36, p. 135–143, 3 2012. ISSN 03645916.

GUO, J.; CHENG, S. sen; CHENG, Z. jian. Characteristics of deoxidation and desulfurization during lf refining al-killed steel by highly basic and low oxidizing slag. *Journal of Iron and Steel Research International*, v. 21, p. 166–173, 2 2014. ISSN 1006706X.

J., S. P.; M, N. D. . K. *Slag Atlas, 2nd ed*. [S.l.: s.n.], 1995.

JUNG, I. H.; ENDE, M. A. V. Computational thermodynamic calculations: Factsage from calphad thermodynamic database to virtual process simulation. *Metallurgical and Materials Transactions B: Process Metallurgy and Materials Processing Science*, Springer, v. 51, p. 1851–1874, 10 2020. ISSN 10735615.

JUNG, I. ho. Calphad : Computer coupling of phase diagrams and thermochemistry overview of the applications of thermodynamic databases to steelmaking processes. *CALPHAD: Computer Coupling of Phase Diagrams and Thermochemistry*, Elsevier Ltd, v. 34, p. 332–362, 2010. ISSN 0364-5916. Disponível em: <http://dx.doi.org/10.1016/j.calphad.2010.06.003>.

KIM, H. et al. The effect of mgo on the viscosity of the cao-sio2-20 wt2o3-mgo slag system. *Steel Research International*, v. 81, p. 261–264, 2010. ISSN 16113683.

KIM, H. et al. Effect of al2o3 and cao/sio2 on the viscosity of calcium-silicate-based slags containing 10 mass pct mgo. *Metallurgical and Materials Transactions B: Process Metallurgy and Materials Processing Science*, v. 44, p. 5–12, 2013. ISSN 10735615.

KONONOV, V. A.; ZEMSKOV, I. I. *HEAT ENGINEERING MODERN HIGH-TEMPERATURE THERMAL INSULATION FOR STEEL-POURING LADLES*. 2012. 20-25 p. Disponível em: <https://link.springer.com/article/10.1007/s11148-012-9484-4>.

KOZAKEVITCH, P. Viscosité des laitiers de hauts fourneaux : laitiers des marches en ferro-manganèse. *Revue de Métallurgie*, v. 64, p. 9–14, 1954. ISSN 0035-1563.

KOZAKEVITCH, P. Viscosité et éléments structuraux des aluminosilicates fondus : laitiers cao-ai2o3-sio2 entre 1 600 et 2 100 °c. *LES MEMOIRES SCIENTIFIQUES DE LA REVUE DE METALLURGIE*, 1960.

KOZAKEVITCH, P.; MISRA, R. Viscosité et fusibilité des laitiers magnésiens aux faibles teneurs en silice. *Revue de Métallurgie*, v. 63, p. 471–476, 1966. ISSN 0035-1563.

LEE, Y. S. et al. Influence of basicity and feo content on viscosity of blast furnace type slags containing feo. *ISIJ International*, v. 44, p. 1283–1290, 2008. ISSN 0915-1559.

LIM, J. W. et al. Overview of steel slag application and utilization. *ICMER 2015*, 2016.

LUZ, A. P. et al. Slag foaming practice in the steelmaking process. *Ceramics International*, Elsevier Ltd and Techna Group S.r.l., v. 44, p. 8727–8741, 2018. ISSN 02728842. Disponível em: <https://doi.org/10.1016/j.ceramint.2018.02.186>.

MACHADO, M. *ELABORAÇÃO, REFINO E LINGOTAMENTO DO AÇO*. 2007. Disponível em: <https://docplayer.com.br/11052283-Elaboracao-refino-e-lingotamento-do-aco.html>.

MACHIN, J. S.; HANNA, D. L. Viscosity studies of system cao–mgo–al2o3–sio2: 1, 40*Journal of the American Ceramic Society*, v. 29, 1945.

MACHIN, J. S.; YEE, T. B. Viscosity studies of system cao-mgo-al2o3-sio2: Ii, cao-al2o3-sio2*. *Journal of the American Ceramic Society*, v. 31, p. 200–204, 1948. ISSN 0002-7820.

MACHIN, J. S.; YEE, T. B. Viscosity studies of system cao-mgo-al2o3-sio2:60 and 65 percent sio2. *Journal of the American Ceramic Society*, v. 37, p. 177–186, 1954.

MACHIN, J. S.; YEE, T. B.; HANNA, D. L. Viscosity studies of system cao–mgo–al2o3–sio2: Iii, 35, 45, and 50*Journal of the American Ceramic Society*, v. 35, p. 322–325, 1952. ISSN 15512916.

MACPHERSON, G. 1.08 - calcium–aluminum-rich inclusions in chondritic meteorites. In: HOLLAND, H. D.; TUREKIAN, K. K. (Ed.). *Treatise on Geochemistry*. Oxford: Pergamon, 2007. p. 1–47. ISBN 978-0-08-043751-4. Disponível em: <https://www.sciencedirect.com/science/article/pii/B0080437516010653>.

MADRUGA, V. da S. *ANÁLISE COMPARATIVA DOS SULFETOS FORMADOS VIA LINGOTAMENTO CONVENCIONAL E VIA LINGOTAMENTO CONTÍNUO NO AÇO SAE 1050*. 2016.

MAZUMDAR, D.; EVANS, J. W. *Modeling of steelmaking processes*. [S.l.]: CRC Press, 2010. 463 p. ISBN 9781439883020.

MEYER. Viscosity of slags in schlema. 2017.

MEYER, I. B. et al. *Viscosity of Slags in Schlema*. 2017.

MILLS, K. C. et al. Round robin project on the estimation of slag viscosities. *Scandinavian Journal of Metallurgy*, p. 396–403, 2001.

MIN, G. U. O.; MEI, Z.; XI-DONG, W. Viscosities behavior of cao-sio2-mgo-al2o3 slag with low mass ratio of cao to sio2 and wide range of al2o3 content. *Journal of Iron and Steel Research International*, Central Iron and Steel Research Institute, v. 18, p. 1–17, 2011. ISSN 1006-706X. Disponível em: <http://dx.doi.org/10.1016/S1006-706X(11)60015-0>.

PELTON, A. D.; BLANDER, M. *Thermodynamic Analysis of Ordered Liquid Solutions by a Modified Quasichemical Approach Application to Silicate Slags*. 1986.

PENGCHENG, L.; XIAOJUN, N. Effects of mgo / al 2 o 3 ratio and basicity on the experiments and modeling. *Metallurgical and Materials Transactions B*, Springer US, v. 47, p. 446–457, 2016. ISSN 1543-1916.

PEREIRA, A. L. et al. *ISO-VISCOSITY CURVES FOR CAO-SIO2-AL2O3-MGO STEELMAKING SLAGS AT HIGH TEMPERATURE **. 2019.

PERSSON, M. *Investigations of slag properties and reactions*. [S.l.]: Materialvetenskap, Kungliga Tekniska hogskolan, 2007. ISBN 9789171786500.

REIS, B. H.; WAGNER, E.; BIELEFELDT, V. *ESTUDO SOBRE A CAPACIDADE DE ABSORÇÃO DE INCLUSÕES PELA ESCÓRIADEREFINO SECUNDÁRIO NA FABRICAÇÃO DE AÇOS*. 2013.

RIHL, D. J. *ESTUDO DA INFLUÊNCIA DO TEMPO DE ESTRIPAMENTO NEGATIVO NA FORMAÇÃO DAS MARCAS DE OSCILAÇÃO E SEUS IMPACTOS EM DEFEITOS SUPERFICIAIS*. 2012.

RIYAHIMALAYERI, K.; ÖLUND, P.; SELLEBY, M. Effect of vacuum degassing on non-metallic inclusions in an asea-skf ladle furnace. *Ironmaking and Steelmaking*, v. 40, p. 470–477, 8 2013. ISSN 03019233.

ROCHA, B. P. *ESTUDO DA VIABILIDADE DA REUTILIZAÇÃO DA ESCÓRIA DO REFINO SECUNDÁRIO NO FORNO ELÉTRICO A ARCO*. 2011.

ROCHA, V. C. et al. Evaluation of secondary steelmaking slags and their relation with steel cleanliness. *Metallurgical and Materials Transactions B: Process Metallurgy and Materials Processing Science*, v. 48, p. 1423–1432, 2017. ISSN 10735615.

ROCHA, V. C. D. *ESTUDO COMPARATIVO ENTRE FLUXANTES APLICADOSNOLINGOTAMENTO CONTÍNUO DO AÇO SAE 1046 MOD*. 2014.

ROCHA, V. C. da. *VISCOSIDADE EFETIVA DE ESCÓRIASE PARÂMETRO CINÉTICO DE AGITAÇÃOAPLICADOS NA LIMPEZAINCLUSIONÁRIA DE AÇOS ESPECIAIS DURANTE DESGASEIFICAÇÃO AVÁCUO*. 2016.

ROCHA, V. C. da. Assessment of viscosity calculation for calcium-silicate based slag using computational thermodynamics. *Metallurgy and materials*, v. 71, p. 243–252, 2018.

ROCHA, V. C. da et al. Effective viscosity of slag and kinetic stirring parameter applied in steel cleanliness during vacuum degassing. *Materials Research*, v. 20, p. 1480–1491, 2017. ISSN 1516-1439.

ROSCOE, R. The viscosity of suspensions of rigid spheres. *British Journal of Applied Physics*, v. 3, p. 267–269, 1952. ISSN 05083443.

ROSSUM, G. V.; JR, F. L. D. *Python reference manual*. [S.l.]: Centrum voor Wiskunde en Informatica Amsterdam, 1995.

SAITO, N. et al. Viscosity of blast furnace type slags. *Metallurgical and Materials Transactions B: Process Metallurgy and Materials Processing Science*, v. 34, p. 509–516, 2003. ISSN 10735615.

SCHUMACHER, K. J.; WHITE, J. F.; DOWNEY, J. P. Viscosities in the calcium–silicate slag system in the range of 1798 k to 1973 k (1525° c to 1700° c). *Metallurgical and Materials Transactions B*, Springer, v. 46, n. 1, p. 119–124, 2015.

SEETHARAMAN, S.; MUKAI, K.; SICHEN, D. U. Viscosities of slags — an overview. *International Conference on Molten Slags Fluxes and Salts*, p. 31–42, 2004.

SEOK, S.-H. Viscosity of highly basic slags. *ISIJI*, 2007.

SHAMSUDDIN, M. *Physical chemistry of metallurgical processes*. [S.l.]: John Wiley & Sons, 2016.

SHANKAR, A. Experimental investigation of the viscosities. *Metallurgical and Materials Transactions B*, v. 38, p. 911–915, 2007.

SILVA, A. L. V. D. C. E. *Non-metallic inclusions in steels - Origin and control*. [S.l.]: Elsevier Editora Ltda, 2018. 283-299 p.

SONG, M.; SHU, Q.; SICHEN, D. Viscosities of the quaternary al2o3-cao-mgo-sio 2 slags. *Steel Research International*, v. 82, p. 260–268, 2011. ISSN 16113683.

SUN, K.-H. *FUNDAMENTAL CONDITION OF GLASS FORMATION**. 1947.

SUZUKI, M.; JAK, E. Quasi-chemical viscosity model for fully liquid slag in the al 2 o 3 -cao-mgo-sio 2 system . part ii : Evaluation of slag viscosities. *Metallurgical and Materials Transactions B*, v. 44, p. 1451–1465, 2013.

TANG, X. long et al. Viscosities behavior of cao-sio2-mgo-al2o3 slag with low mass ratio of cao to sio2 and wide range of al2o3 content. *Journal of Iron and Steel Research International*, Central Iron and Steel Research Institute, v. 18, p. 1–17, 2011. ISSN 1006706X. Disponível em: <http://dx.doi.org/10.1016/S1006-706X(11)60015-0>.

URBAIN, G.; BOTTINGA, Y.; RICHET, P. Viscosity of liquid silica, silicates and alumino-silicates. *Geochimica et Cosmochimica Acta*, v. 46, p. 1061–1072, 1982. ISSN 00167037.

WANG, W. et al. Viscosity and structure of mgo–sio2-based slag melt with varying b2o3 content. *Ceramics International*, Elsevier Ltd and Techna Group S.r.l., v. 46, p. 3631–3636, 2020. ISSN 02728842. Disponível em: <https://doi.org/10.1016/j.ceramint.2019.10.082>.

XU, J.-F. et al. Viscosity of low silica cao–5mgo–al2o3–sio2 slags. *Ironmaking & Steelmaking*, Taylor Francis, v. 41, n. 7, p. 486–492, 2014. Disponível em: <https://doi.org/10.1179/1743281213Y.0000000142>.

XU, L. S. D. C. J. Experimental investigation on viscosity of cao-mgo(-alo)-sio slags and solid-liquid mixtures. *Journal of Iron and Steel Research, International*, v. 22(12), p. 1091–1097, 2015.

ZANON, E. B. *DETERMINAÇÃO EXPERIMENTAL E SIMULAÇÃO TERMODINÂMICA DAS FASES PRESENTES EM ESCÓRIAS DE REFINO SECUNDÁRIO DE AÇOS*. 2013.

ZHANG, G.-H.; CHOU, K.-C. Influence of al2o3/sio2 ratio on viscosities of cao-al2o3-sio2 melt. *ISIJ International*, v. 53, p. 177–180, 2013. ISSN 0915-1559. Disponível em: <http://japanlinkcenter.org/DN/JST.JSTAGE/isijinternational/53.177?lang=en&from=CrossRef&type=abstract>.